

UNCLASSIFIED

AD 448909

DEFENSE DOCUMENTATION CENTER

FOR

SCIENTIFIC AND TECHNICAL INFORMATION

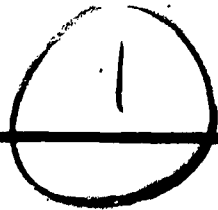
CAMERON STATION ALEXANDRIA, VIRGINIA



UNCLASSIFIED

NOTICE: When government or other drawings, specifications or other data are used for any purpose other than in connection with a definitely related government procurement operation, the U. S. Government thereby incurs no responsibility, nor any obligation whatsoever; and the fact that the Government may have formulated, furnished, or in any way supplied the said drawings, specifications, or other data is not to be regarded by implication or otherwise as in any manner licensing the holder or any other person or corporation, or conveying any rights or permission to manufacture, use or sell any patented invention that may in any way be related thereto.

REPORT 351



REPORT 351

ADVISORY GROUP FOR AERONAUTICAL RESEARCH AND DEVELOPMENT

64 RUE DE VARENNE, PARIS VII

APRIL 1961

09

THE INFLUENCE OF AEROELASTICITY  
ON THE LONGITUDINAL STABILITY  
OF A SWEEP WING SUBSONIC  
TRANSPORT AIRCRAFT

by

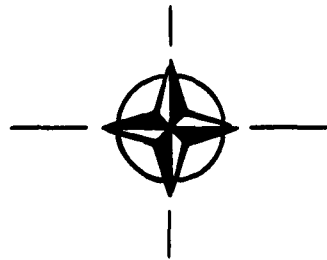
C. M. KALKMAN

REPORT 351

AD No. 48909  
DDC FILE COPY



448909



DDC  
RECEIVED  
OCT 7 - 1961  
AGENCY

NORTH ATLANTIC TREATY ORGANISATION

67-08-5071

14 → REPORT 351  
no.

~~NORTH ATLANTIC TREATY ORGANIZATION~~

5 → ADVISORY GROUP FOR AERONAUTICAL RESEARCH AND DEVELOPMENT,  
*Paris (France).*

6 → THE INFLUENCE OF AEROELASTICITY ON THE LONGITUDINAL  
STABILITY OF A SWEEP WING SUBSONIC  
TRANSPORT AIRCRAFT,

10 by  
C.M. Kalkman

11 → April 61

14

This Report is one in the Series 334-374, inclusive, presenting papers, with discussions, given at the AGARD Specialists' Meeting on 'Stability and Control', Training Center for Experimental Aerodynamics, Rhode-Saint-Genèse, Belgium, 10-14 April 1961, sponsored jointly by the AGARD Fluid Dynamics and Flight Mechanics Panels



## SUMMARY

A numerical treatment of the influence of the aeroelastic deformations on the longitudinal stability and control characteristics of an aircraft with a swept-back wing of large aspect ratio is carried out for the sub-critical speed range. Only the deformation of the wing and the bending of the fuselage have been taken into consideration.

The method used to calculate the deformations of the wing is based on the superposition of a number of pre-selected load distributions (*A Superposition Method for Calculating the Aeroelastic Behavior of Swept Wings*, Aug. 1951, by R.B. Brown et alii). An investigation of the accuracy of the method has been made by comparing the numerical results with those of another more exact method which proved the reliability of the present method.

As a result of the study it was found that the stability and control of the aircraft are only slightly affected by the aeroelastic deformation.

## SONMAIRE



Un traitement numérique de l'influence des déformations aéroélastiques sur la stabilité longitudinale et sur les caractéristiques de contrôle d'un avion à voilure en flèche, d'allongement élevé, est effectué en ce qui concerne la gamme des vitesses sous critiques. Seules la déformation de la voilure et la flexion du fuselage ont été prises en considération.

Le mode de calcul des déformations alaires utilisé se base sur la superposition d'un certain nombre de répartitions des charges prédéterminés (*A Superposition Method for Calculating the Aeroelastic Behavior of Swept Wings*, Aug. 1951, by R.B. Brown et alii). La précision de ce mode a été vérifiée en confrontant les résultats numériques obtenus et ceux obtenus d'après un autre mode plus précis, ce qui a permis de mettre en évidence la sûreté du mode actuellement employé.

Par suite de cette étude il a été constaté que la stabilité et le contrôle de l'avion ne sont que peu sensibles à la déformation aéroélastique.

533.6.013.42  
533.6.013.412

3c2c1a1  
3c6b2

## CONTENTS

|  | Page |
|--|------|
| SUMMARY  | ii   |
| LIST OF TABLES   | v    |
| LIST OF FIGURES  | v    |
| NOTATION   | vi   |
| 1. INTRODUCTION  | 1    |
| 2. STATEMENT OF THE PROBLEM  | 1    |
| 3. METHODS TO DETERMINE THE AERODYNAMIC LOADS ON ELASTIC WINGS   | 3    |
| 3.1 General  | 3    |
| 3.2 The Superposition Method   | 3    |
| 3.2.1 Description of the Method  | 3    |
| 3.2.2 The Calculation of the Superposition<br>Coefficients ( $A_s$ , $B_s$ and $C_s$ )   | 5    |
| 4. CALCULATION OF THE AERODYNAMIC LOADING ON THE RIGID WING  | 6    |
| 5. CALCULATION OF THE DEFORMATIONS DUE TO A GIVEN<br>AERODYNAMIC LOADING   | 7    |
| 6. CALCULATION OF THE DOWNWASH OF THE ELASTIC WING AT THE<br>HORIZONTAL TAIL   | 10   |
| 7. FUSELAGE BENDING  | 13   |
| 8. THE 'EXACT' METHOD TO CALCULATE THE DISTRIBUTION OF THE<br>AERODYNAMIC LOADING OF AN ELASTIC WING   | 14   |
| 9. COMPARISON OF THE RESULTS OF WING LOAD CALCULATIONS WITH<br>THE SUPERPOSITION METHOD AND THE 'EXACT' METHOD                                 | 15   |
| 10. INVESTIGATION OF THE INFLUENCE OF AEROELASTICITY ON THE<br>STATIC LONGITUDINAL STABILITY OF AN AIRCRAFT WITH<br>SLENDER SWEEPED-BACK WINGS | 17   |
| 10.1 Basic Data for the Calculation  | 17   |
| 10.2 Survey of the Calculations  | 18   |
| 10.3 Results   | 18   |
| 11. CONCLUSIONS  | 21   |
| REFERENCES   | 23   |
| TABLES   | 24   |

**FIGURES**

**ADDENDUM: Complete List of Papers in Series**

**DISTRIBUTION**

## LIST OF TABLES

|           |   | Page |
|-----------|---|------|
| TABLE I   | Flight Conditions Used for Deformation Calculations<br>(see Sec.10.1) | 24   |
| TABLE II  | Numerical Values of $(x_{c.g.} - x_{c.p.})/\bar{c}$                   | 24   |
| TABLE III | Values of $d\epsilon/d\alpha$ for the rigid and the Elastic Wing      | 24   |
| TABLE IV  | Cases Considered (see Sec.10.2)                                       | 25   |

## LIST OF FIGURES

|        |   |    |
|--------|---|----|
| Fig. 1 | Load distributions for compressible and incompressible flow determined by the superposition method and by the exact method            | 26 |
| Fig. 2 | Pitching moment distributions for compressible and incompressible flow determined by the superposition method and by the exact method | 27 |
| Fig. 3 | Superposition of angle-of-attack distributions ( $\alpha_T$ ) and comparison of results with those of exact method                    | 28 |
| Fig. 4 | Elevator deflection as a function of $C_L$ ( $C_{M_f} = 0$ )  | 29 |
| Fig. 5 | Elevator deflection as a function of $C_L$<br>( $C_{M_f} = -0.015/\sqrt{1 - M^2}$ )   | 30 |
| Fig. 6 | Shift of centre of pressure to aeroelasticity, with and without compressibility effects   | 31 |
| Fig. 7 | Influence of compressibility and aeroelasticity on wing lift gradient   | 32 |
| Fig. 8 | Influence of compressibility and aeroelasticity on wing lift gradient   | 33 |
| Fig. 9 | Manoeuvre margins stick-fixed   | 34 |
| Fig.10 | Elevator travel per 'g'   | 35 |
| Fig.11 | Vertical displacement of wing tip with corresponding distributions of circulation   | 36 |

## NOTATION

|                          |  |
|--------------------------|--|
| $A$                      | lift gradient, $\text{rad}^{-1}$   |
| $A_t$                    | lift gradient of horizontal tail, $\text{rad}^{-1}$  |
| $A_{tR}$                 | lift gradient of horizontal tail for the aircraft with rigid fuselage, $\text{rad}^{-1}$   |
| $A_s, B_s, C_s$          | 'superposition'-coefficients (see Sec.3.2)   |
| $a_1, b_1, c_1$          | coefficients of cubic equations in $\eta$ , approximating elastic angle-of-attack distributions $\alpha_{F1}(\eta_1)$ caused by final loading due to $\alpha_{F1}$ (Eqn.(6)) |
| $B_0$                    | bending stiffness at wing root ( $= EI_0$ ), $\text{kgm}^2$  |
| $B$                      | bending stiffness in arbitrary section $y$ ( $= EI$ ), $\text{kgm}^2$  |
| $b$                      | wing span, $m$   |
| $B_{f_0}$                | bending stiffness of fuselage at c.g. section ( $= EI_{f_0}$ ), $\text{kgm}^2$   |
| $C_{M_R}$                | rigid-wing pitching moment coefficient   |
| $C_M$                    | wing pitching-moment coefficient   |
| $C_m$                    | local pitching-moment coefficient  |
| $C_L$                    | total lift coefficient   |
| $C_{L_W}$                | wing lift coefficient  |
| $C_l$                    | local lift coefficient   |
| $C_{M_f}$                | fuselage pitching moment coefficient at $C_L = 0$  |
| $\bar{c}$                | mean aerodynamic chord, $m$  |
| $c$                      | local chord, $m$   |
| $c_0$                    | root chord, $m$  |
| $E$                      | modulus of elasticity, $\text{kg/m}^2$   |
| $H_m$                    | manoeuvre margin, stick fixed  |
| $I$                      | wing section moment of inertia, $m^4$  |
| $i_{11}, i_{12}, i_{22}$ | influence functions of wing (Eqn.(24))   |

|                                |  |
|--------------------------------|--|
| $ky_1$                         | load per unit length $y$ at section $y_1$ , kg/m   |
| $l_t$                          | tail length = fuselage length, distance of c.g. to a.c. of horizontal tailplane m  |
| $my_1$                         | pitching moment per unit length $y$ at section $y_1$ , kg  |
| $M_x, M_y$                     | projections of moment vector on X-axis and Y-axis respectively, kgm  |
| $M$                            | Mach number  |
| $n$                            | number of 'Multhopp' pivotal points  |
| $P$                            | compressibility factor (Eqn. (13))   |
| $Q_{11}$                       | $= \frac{1}{B \cos^2 \theta}$  |
| $Q_{22}$                       | $= \frac{1}{T} + \frac{1}{B} \tan^2 \theta$  |
| $Q_{21}$                       | $= Q_{12} = - \frac{1 \tan \theta}{B \cos \theta}$   |
| $q$                            | dynamic pressure ( $= \frac{1}{2} \rho V^2$ ), kg/m <sup>2</sup>   |
| $S$                            | wing area, m <sup>2</sup>  |
| $S_t$                          | area of horizontal tail, m <sup>2</sup>  |
| $V$                            | airspeed, m/sec  |
| $v_{c.g.}$                     | 'tail volume' of horizontal tail with reference to c.g.  |
| $v_{a.c.}$                     | $= v_{c.g.} + \frac{x_{c.g.} - x_{a.c.}}{\bar{c}} \frac{S_t}{S}$   |
| $v_t$                          | $= \frac{v_{a.c.}}{1 + \frac{A_t S_t}{A S} \left(1 - \frac{d\epsilon}{d\alpha}\right)}$  |
| $W$                            | weight of aircraft, kg   |
| $x_{c.p.}; x_{c.g.}; x_{a.c.}$ | distances from c.p., c.g. and a.c. to apex of swept wing, respectively, m  |
| $y$                            | wing co-ordinate measured along elastic axis of wing, m  |
| $y'$                           | wing co-ordinate measured along elastic axis of wing, measured along normal on plane of symmetry in point of intersection with elastic axis, m |

|                        |   |
|------------------------|---|
| $Z_{tip}$              | $= Z_{1=13}$ , vertical displacement of wing tip, m                 |
| $\alpha$               | wing angle of attack, rad   |
| $\alpha_I$             | angle-of-attack distribution along unloaded wing, rad               |
| $\alpha_E$             | deformation of angle-of-attack distribution, rad                    |
| $\alpha_F$             | final angle-of-attack distribution $(= \alpha_E + \alpha_I)$ , rad  |
| $\gamma$               | dimensionless lift coefficient $(= \frac{1}{2} C_l c/b)$            |
| $\mu$                  | dimensionless pitching-moment coefficient $(= \frac{1}{2} C_m c/b)$ |
| $\varphi_x, \varphi_y$ | angles of rotation around X-axis and Y-axis respectively, rad       |
| $\theta$               | angle of sweep of elastic axes, rad                                 |
| $\eta$                 | $= y'/\frac{1}{2}b = 2y \cos \theta/b$                              |
| $\psi$                 | $= bg \cos \eta$ ( $\psi = 0$ at wing tip), rad                     |
| $\lambda$              | aspect ratio of wing  |
| $\Gamma$               | $= V b \gamma$ , $m^2 \text{sec}^{-1}$                              |
| $\delta_t$             | deflection of all-movable horizontal tail, deg.                     |
| $\epsilon$             | downwash angle, rad   |

**THE INFLUENCE OF AEROELASTICITY ON THE LONGITUDINAL  
STABILITY OF A SWEEPED WING SUBSONIC  
TRANSPORT AIRCRAFT**

C.M. Kalkman\*

**1. INTRODUCTION**

By order of the 'Netherlands Aircraft Development Board', a quantitative calculation was carried out for a hypothetical aircraft with elastic swept-back wings in order to investigate the changes in the longitudinal stability and control characteristics as a consequence of the deformations. Only the influences of wing deflection and fuselage bending are taken into account.

The determination of the load distribution on the elastic wing under consideration has been performed by the method of superposition. Many other methods of calculation may be found in the literature on this subject; most are complicated and time-consuming. The method of superposition is relatively simple, so that it seemed desirable to investigate its reliability from the point of view of accuracy. The influence of compressibility of the air was introduced into the calculation by an approximate expression. To avoid too much numerical calculation the reliability of the method of superposition was checked at only one Mach number ( $M = 0.8$ ).

With the help of the method of superposition the distributions of lift and pitching moment along the elastic wing are determined for various values of  $M$  and the dynamic pressure (horizontal flight at two altitudes). With these data the quantities which are of importance for the static longitudinal stability and control, e.g. location of the centre of pressure and lift gradient, are determined. Moreover, the downwash at the horizontal tail is calculated by using the distribution of lift along the span of the elastic wing.

With the parameters obtained in this way, elevator angles to trim in level flight, elevator deflections per 'g', and the corresponding manoeuvre margins were calculated as functions of speed. To be able to detect the aeroelastic effects these calculations were carried out for the rigid aircraft and the flexible aircraft with and without taking into account the influence of compressibility of the air.

**2. STATEMENT OF THE PROBLEM**

The purpose of this investigation is to determine to what extent the static longitudinal stability and control characteristics of an aircraft with slender swept-back wings are affected by aeroelastic deformations. The behaviour of large transports and bombers was of primary interest in this respect as large effects are to be expected in these cases.

---

\* *Nationaal Luchtvaartlaboratorium, Amsterdam, Netherlands*

To get an impression of the quality and magnitude of the above-mentioned factors quantitative calculations were carried out for a hypothetical aircraft, the shape and dimensions of which roughly agree with those of the Boeing B-47. In order to limit the scope of the calculations to a reasonable extent only wing deflections and aeroelastic fuselage bending are considered.

For this purpose the aircraft was supposed to consist of the following parts:

- (a) An elastic wing without twist with a symmetrical cross-section and an angle of sweep of the quarter-chord line  $\theta = 35^\circ$ , an aspect ratio  $\lambda = 8$  and a taper ratio of 1/3. The corresponding wing area amounts to 162 m<sup>2</sup>;
- (b) A flexible fuselage of about 20 m length;
- (c) A rigid all-movable tail with  $\theta_{1/4c} = 35^\circ$  and  $\lambda = 4$  (area = 25 m<sup>2</sup>).

The separate effects of deformation may be compared by combining a rigid wing with a flexible fuselage and a flexible wing with a rigid fuselage. Moreover, the influence of compressibility has been taken into account; but only sub-critical Mach numbers have been considered.

A general view of the problems, which present themselves successively when calculating the aeroelastic influence on longitudinal stability, may be obtained most effectively with the help of the pitching-moment equation for the equilibrium condition. This equation can be approximately expressed as follows:

$$v_t A_t \delta_t = C_{M_f} + \frac{(x_{c.g.} - x_{a.c.})}{\bar{c}} C_L - v_t \frac{A_t}{A} \left(1 - \frac{d\epsilon}{d\alpha}\right) C_L \quad (1)$$

where

$$v_t = \frac{v_{a.c.}}{1 + \frac{A_t}{A} \frac{S_t}{S} \left(1 - \frac{d\epsilon}{d\alpha}\right)} \quad (2)$$

and

$$v_{a.c.} = v_{c.g.} + \frac{x_{c.g.} - x_{a.c.}}{\bar{c}} \frac{S_t}{S} \quad (3)$$

The lift gradient  $A$  of the wing and of the horizontal tail  $A_t$ , the location of the wing centre of pressure  $x_{a.c.}/\bar{c}$  and the downwash gradient  $d\epsilon/d\alpha$  are considered to be affected by aeroelastic deformation in Equation (1). If it is possible to calculate these quantities for different values of Mach number and dynamic pressure the effects of deformation of wing and fuselage can be determined immediately.

A discussion of the applied calculation methods will be given in the following sections.

### 3. METHODS TO DETERMINE THE AERODYNAMIC LOADS ON ELASTIC WINGS

#### 3.1 General

The difficulty which presents itself when calculating aerodynamic loads on lifting surfaces is a consequence of the mutual influence of load and deformation. Most existing methods have the disadvantage that complicated iteration procedures are necessary to determine the equilibrium condition of the structure. Moreover, these methods are often based on 'strip theory', so that induced aerodynamic effects are not taken into account.

In Reference 1 a method is given - the so-called 'superposition method' - which leads rapidly to the required results. Since the accuracy of this method is somewhat adversely affected by the way, in which the influence of compressibility is taken into account, a second more exact method is applied. By comparing the numerical results of these two methods the feasibility of the superposition method can be judged.

#### 3.2 The Superposition Method

##### 3.2.1 Description of the Method

Although it is rather difficult to calculate the final angle-of-attack distribution for a wing with a given initial (unloaded)  $\alpha$ -distribution, it is quite possible to calculate the angle-of-attack distribution for the unloaded condition if the final angle-of-attack distribution (or final loading) is given. This reverse procedure is the basis of the superposition method.

Starting from a number of arbitrarily selected final angle-of-attack distributions ( $\alpha_F$ ), the load distributions for the wing, considered to be rigid in this condition, are now calculated. The deformations ( $\alpha_E$ ) which are a consequence of these calculated loadings may be determined if the stiffness parameters of the wing are known.

The angle-of-attack distribution  $\alpha_I$  of the unloaded wing then follows from:

$$\alpha_F = \alpha_I + \alpha_E \quad (4)$$

This relation applies to any wing section. From each selected distribution of the final angle of attack ( $\alpha_F$ ) follows a corresponding one along the unloaded wing.

A number of  $\alpha_F$ -distributions are considered now from which the corresponding  $\alpha_I$ -distributions are calculated. The given  $\alpha_I$ -distribution may then be approximated by the following expression:

$$\alpha_I = A_S \alpha_{I_1} + B_S \alpha_{I_2} + C_S \alpha_{I_3} + \dots \quad (5)$$

In general the following four  $\alpha_F$ -distributions are chosen:

- (a) A distribution  $\alpha'_I$  equal to the given  $\alpha_I$ -distribution;
- (b) Three additional distributions  $\alpha_{P_1}$ ,  $\alpha_{P_2}$  and  $\alpha_{P_3}$ , proportional respectively to  $\eta$ ,  $\eta^2$  and  $\eta^3$  ( $\eta = (2y/b) \cos \theta$ , the dimensionless coordinate).

The resulting aerodynamic loadings cause the elastic deformations of the angle-of-attack distributions  $\alpha'_E$  and  $\alpha_{E_i}$  ( $i = 1$  to 3), which may be approximated by the following cubic equations in  $\eta$ :

$$\left. \begin{aligned} \alpha_{E_i} &= qP(a_i\eta + b_i\eta^2 + C_i\eta^3) \\ \alpha'_E &= qP(a\eta + b\eta^2 + c\eta^3) \end{aligned} \right\} \quad (6)$$

These equations show moreover that  $\alpha_E$  is linearly dependent on the dynamic pressure  $q$  and the quantity  $P$ , which represents the ratio between the lift gradients with and without compressibility effects. The relation between  $\alpha_E$  and  $P$  is based on the assumption that the load distribution does not change shape with increasing speed below the critical speed. This assumption, which is made in Reference 1 without motivation, appeared to be acceptable according to comparative numerical results.

Furthermore, if we suppose that Hooke's law applies and that the aerodynamic loading is linearly dependent on the angle of attack, the following relations may be derived from Equations (4) and (5):

$$\left. \begin{aligned} \alpha_E &= A_S\alpha_{E_1} + B_S\alpha_{E_2} + C_S\alpha_{E_3} + \dots \\ \alpha_P &= A_S\alpha_{P_1} + B_S\alpha_{P_2} + C_S\alpha_{P_3} + \dots \end{aligned} \right\} \quad (7)$$

As  $A_S$ ,  $B_S$ ,  $C_S$ , ..... follow from the approximation given by Equation (5) the final angle-of-attack distribution can now be determined by starting from a given  $\alpha_I$ -distribution; the resulting aerodynamic properties may then be derived.

The given  $\alpha_I$ -distribution is now composed, according to Equation (5), in the following way of the  $\alpha_I$ -distributions corresponding with  $(\alpha_{P_i} + \alpha_{P_1})$ :

$$A_S\alpha_{I_1} + B_S\alpha_{I_2} + C_S\alpha_{I_3} + \alpha'_I = \alpha_I \quad (8)$$

where

$$\alpha'_I = \alpha_I \quad (9)$$

With the help of Equations (4) and (9), Equation (8) may be transformed into

$$A_S\alpha_{I_1} + B_S\alpha_{I_2} + C_S\alpha_{I_3} = \alpha'_E \quad (10)$$

With this relation the 'superposition coefficients' may be calculated along the lines given in the next section.

Once the coefficients  $A_S$ ,  $B_S$  and  $C_S$  are known, the quantities which are of importance for this investigation, viz. wing lift gradient, wing pitching moment and downwash gradient at the tail, may be calculated from the following equations:

$$\left. \begin{aligned} A &= A_R + A_S C_{L_1} + B_S C_{L_2} + C_S C_{L_3} \\ C_M &= C_{M_R} + A_S C_{M_1} + B_S C_{M_2} + C_S C_{M_3} \\ \frac{d\epsilon}{d\alpha} &= \left(\frac{d\epsilon}{d\alpha}\right)_R + A_S \left(\frac{d\epsilon}{d\alpha}\right)_1 + B_S \left(\frac{d\epsilon}{d\alpha}\right)_2 + C_S \left(\frac{d\epsilon}{d\alpha}\right)_3 \end{aligned} \right\} \quad (11)$$

The first terms on the right-hand sides of these equations represent the coefficients of lift gradient, pitching moment and downwash gradient respectively at the horizontal tail for the rigid wing. The second, third and fourth terms refer to the corresponding quantities occurring as a consequence of the selected  $\alpha$ -distributions along the rigid wing span ( $\alpha = \eta, \eta^2$  and  $\eta^3$ ) and may be considered as correction terms.

### 3.2.2 The Calculation of the Superposition Coefficients ( $A_S$ , $B_S$ and $C_S$ )

The superposition coefficients  $A_S$ ,  $B_S$  and  $C_S$  must be derived from Equation (10) as mentioned in the preceding section. To get an expression for the  $\alpha_I$ -distributions the corresponding deformations  $\alpha_{E_1}$  should be calculated from the loading caused by the selected distributions  $\alpha_{P_1}$ . In agreement with the fact that these  $\alpha_{P_1}$ -distributions are of the third degree at most ( $\alpha_{P_1} = \eta, \eta^2$  and  $\eta^3$ ) the number of superposition coefficients does not amount to more than three. The elastic angle-of-attack distributions  $\alpha_{E_1}$  have been approximated by cubic equations in  $\eta$ :

$$\alpha_{E_1} = qP(a_1\eta + b_1\eta^2 + c_1\eta^3) \quad (12)$$

The product  $qP$  is dependent on flight altitude and Mach number. For this investigation two altitudes (1000 m and 10,000 m) and a Mach number range up to 0.8 have been considered (sub-critical speeds).

The influence of compressibility is expressed by the quantity  $P$ , the ratio of the lift gradients approximated according to Reference 3 for rigid wings in compressible and incompressible flow:

$$P = \frac{(A_T)_M}{(A_T)_{M=0}} = \frac{\lambda + 2 \cos \theta}{\lambda \sqrt{1 - M^2 \cos^2 \theta} + 2 \cos \theta} \quad (13)$$

The angle-of-attack distributions  $\alpha_{I_1}$  can now be calculated with the help of Equation (4):

$$\alpha_{P_1} = \alpha_{I_1} + \alpha_{E_1}$$

Inserting the above-mentioned expressions for  $\alpha_{E_1}$  and  $\alpha_{P_1}$  as functions of  $\eta$  leads to:

$$\left. \begin{aligned} \alpha_{I_1} &= \eta - \alpha_{E_1} = (1 - a_1 qP)\eta - b_1 qP\eta^2 - c_1 qP\eta^3 \\ \alpha_{I_2} &= \eta^2 - \alpha_{E_2} = -a_2 qP\eta + (1 - b_2 qP)\eta^2 - c_2 qP\eta^3 \\ \alpha_{I_3} &= \eta^3 - \alpha_{E_3} = -a_3 qP\eta - b_3 qP\eta^2 + (1 - c_3 qP)\eta^3 \end{aligned} \right\} \quad (14)$$

The quantity  $\alpha'_E$  derived from  $\alpha'_P (= \alpha_I)$  should be approximated by a cubic in  $\eta$  as well as the quantities  $\alpha_{E_i}$ :

$$\alpha'_E = a\eta + b\eta^2 + c\eta^3 \quad (15)$$

Equating (10)

$$A_s \alpha_{I_1} + B_s \alpha_{I_2} + C_s \alpha_{I_3} = \alpha'_E$$

and Equation (15) for any value of  $\eta$  leads to:

$$\left. \begin{aligned} A_s \left( \frac{1}{qP} - a_1 \right) - B_s a_2 - C_s a_3 &= a \\ -A_s b_1 + B_s \left( \frac{1}{qP} - b_2 \right) - C_s b_3 &= b \\ -A_s c_1 - B_s c_2 + C_s \left( \frac{1}{qP} - c_3 \right) &= c \end{aligned} \right\} \quad (16)$$

From these equations the unknown quantities  $A_s$ ,  $B_s$  and  $C_s$  can be determined for each combination of altitude and Mach number.

#### 4. CALCULATION OF THE AERODYNAMIC LOADING ON THE RIGID WING

To determine the deformations ( $\alpha_{E_i}$ ) it is necessary to know the loadings caused by the selected distributions of the final angle of attack  $\alpha_{P_1}$  along the span of the wing (considered to be infinitely stiff). There are different methods available to calculate these lift distributions. The method developed by Muthopp<sup>2</sup> has been used for the present investigation. An important advantage of this method compared with most others of the same reliability from the point of view of accuracy is the relatively small extent of the required computational work. This is, among other things, due to a correct selection of the location of the so-called pivotal points

on the lifting surface. In this respect the number of coefficients of the summation terms representing the downwash integral is reduced considerably, if the pivotal points along the span are selected in such a way as to form the projections of the points obtained by dividing the half circle on the wing span into equal parts.

The number of pivotal points ( $m$ ) applied in this investigation amounted to 25, according to Multhopp's recommendation (wing aspect ratio  $\lambda \approx 8$ ):

$$m > 3\lambda\sqrt{1 - M^2} \quad (17)$$

The method results in a number of linear equations with the local lift and the local pitching moment as unknowns.

Apart from the smaller amount of computational work this method also has the advantage that it applies to the swept-back wing and that it is accessible to compressibility calculations. When applying the superposition method use was made exclusively of the results for the incompressible airflow condition, while the 'exact' method carried out for comparative purposes (at  $M = 0.8$ ) was based on Multhopp's method for the compressible case.

#### 5. CALCULATION OF THE DEFORMATIONS DUE TO A GIVEN AERODYNAMIC LOADING

Computation of the aerodynamic loading mentioned in the preceding section provides values for the dimensionless lift per unit length of wing span and for the pitching moment at the pivotal points. With these data the resulting deformations may be calculated. An oblique co-ordinate system was chosen for this purpose, being most suitable for the swept-back wing configuration. The X-axis coincides with the axis of symmetry of the wing and the Y-axis with the elastic axis, which is supposed to be a straight line.

The deformation of the wing may be given by the following differential equations:

$$\left. \begin{aligned} \frac{\partial \varphi_x}{\partial y} &= Q_{11}M_x + Q_{12}M_y \\ \frac{\partial \varphi_y}{\partial y} &= Q_{21}M_x + Q_{22}M_y \end{aligned} \right\} \quad (17)$$

The angles  $\varphi_x$  and  $\varphi_y$  represent the rotations around the X-axis and the Y-axis respectively in an arbitrary section  $y$  of the wing. They are components along the X- and Y-axis of the resulting rotation  $\varphi$ , while  $M_x$  and  $M_y$  are the normal projections on these axes of the resulting moment vector acting at this section. Accordingly the coefficients  $Q_{11}$  in Equation (17) can be expressed as follows:

$$\begin{aligned}
 Q_{11} &= \frac{1}{B \cos^2 \theta} \\
 Q_{22} &= \frac{1}{T} + \frac{1}{B} \tan^2 A \\
 Q_{12} &= Q_{21} = -\frac{1}{B} \frac{\tan A}{\cos \theta}
 \end{aligned}
 \tag{18}$$

The quantities  $B$  and  $T$  represent the bending and torsional stiffnesses respectively of a section normal to the elastic axis, of which the angle of sweep is equal to  $\theta$ . To make a numerical evaluation of the deformations possible, certain assumptions referring to the stiffnesses of the wing had to be made. From a rough estimation of the bending stiffness ( $B_0 = EI_0$ ) at the wing root followed  $B_0 = 10^{12}$  kgcm<sup>2</sup>. The desired data were partly derived from publications on the Boeing B-47 aircraft and partly obtained from estimations on a theoretical base.

In order to realise a reasonably perceptible deformation of the lifting surface it was supposed that the bending stiffness along the span of the tapered wing varied proportionally to the fifth degree of the chord (taper ratio of the wing is equal to 1/3). Furthermore, the assumption was made that for each wing section the ratio of bending stiffness to torsional stiffness ( $T$ ) is constant (a practical value of  $B/T = 4$  has been chosen).

The first equation in (17) is related to the bending of the lifting surface (around the X-axis) while the second equation refers to the change in the angle of attack. Since only the latter is of importance with respect to this investigation attention will be mainly confined to this equation.

The moment  $M_x$  in the section  $y$  may be represented by the following relation:

$$M_x = \int_y^{(b/2)/\cos \theta} k_{y_1} (y_1 - y) \cos \theta \, dy_1 \quad (y < y_1) \tag{19}$$

where  $k_{y_1}$  is the loading per unit length (Y-axis) at the section  $y_1$ . The expression under the integral sign gives the moment of the loading of a wing strip  $y_1$  around an axis in the section  $y$  parallel to the X-axis.

Accordingly the moment  $M_y$  in the section  $y$  may be expressed by:

$$M_y = \int_y^{(b/2)/\cos \theta} m_{y_1} \, dy_1 \tag{20}$$

where  $m_{y_1}$  is the moment around the Y-axis per unit length along this axis in the section  $y_1$ . The moments following from calculations according to Multhopp are

referred to an axis through the quarter-chord point of the section and normal to the plane of symmetry of the wing. Consequently, these moments should be reduced to that point of the section where it is intersected by the elastic axis; furthermore they should be multiplied by  $\cos \theta$  before they can be substituted in Equation (20).

Substituting Equations (19) and (20) in the second Equation in (17), while the co-ordinates  $y$  and  $y_1$  are made dimensionless  $[(2y \cos \theta)/b = \eta]$ , the following expression may be developed:

$$\frac{\partial \varphi}{\partial y} = \frac{-b^2 \tan \theta}{4B \cos^2 \theta} \int_{\eta}^1 k_{\eta_1} (\eta_1 - \eta) d\eta_1 + \frac{b}{2 \cos \theta} \left( \frac{1}{T} + \frac{1}{B} \tan^2 \theta \right) \int_{\eta}^1 m_{\eta_1} d\eta_1 \quad (\eta < \eta_1) \quad (21)$$

Suppose that, according to the above, the bending and torsional stiffnesses vary along the span as the fifth degree of the chord, and taking a taper ratio of 1/3 gives, we obtain:

$$\left. \begin{aligned} B &= B_0 (1 - 2/3 \eta)^5 \\ T &= T_0 (1 - 2/3 \eta)^5 \end{aligned} \right\} \quad (22)$$

Integration of Equation (21) yields:

$$\begin{aligned} \varphi_{\eta}(\eta) &= - \frac{b^3 \tan \theta}{8B_0 \cos^3 \theta} \int_0^{\eta} \left\{ \int_{\eta}^1 k_{\eta_1} (\eta_1 - \eta) d\eta_1 \right\} \frac{d\eta}{(1 - 2/3 \eta)^5} + \\ &+ \frac{b^2}{4 \cos^2 \theta} \left( \frac{1}{T_0} + \frac{1}{B_0} \tan^2 \theta \right) \int_0^{\eta} \left\{ \int_{\eta}^1 m_{\eta_1} d\eta_1 \right\} \frac{d\eta}{(1 - 2/3 \eta)^5} \end{aligned} \quad (23)$$

This equation can be integrated by using influence functions. For the sake of brevity only the final result is presented here:

$$\left. \begin{aligned} a_{\mathbb{E}}(\eta) &= \varphi_{\eta}(\eta) \cos \theta \\ \{a_{\mathbb{E}}(\eta)\}_k &= - \frac{\pi b^4 q \tan \theta}{96 B_0 \cos^2 \theta} \sum_{j=1}^n (i_{21})_{kj} \gamma_j + \\ &+ \frac{\pi}{48} q b^3 c_0 \left( \frac{1}{T_0} + \frac{1}{B_0} \tan^2 \theta \right) \sum_{j=1}^n (i_{22})_{kj} (\mu_j + 0.1 \gamma_j) \left( 1 - \frac{2}{3} \cos \psi_j \right) \end{aligned} \right\} \quad (24)$$

The influence functions  $i_{21}$  and  $i_{22}$  are expressed in the spanwise co-ordinate  $\psi$  ( $\eta = \cos \psi$ ) to allow immediate multiplication with Multhopp's dimensionless coefficients for local lift and pitching moment  $\gamma$  and  $\mu$ . The relation between these coefficients is given by:

$$\left. \begin{aligned} (k_{\eta_1})_j &= 2qb\gamma_j \\ (m_{\eta_1})_j &= 2qbc(\mu + 0.1\gamma)_j \cos \theta \end{aligned} \right\} \quad (25)$$

For an arbitrary section parallel to the plane of symmetry the chord is given by:

$$c_j = c_0 \left( 1 - \frac{2}{3} \cos \psi_j \right) \quad (26)$$

Finally the influence functions occurring in Equation (24) can be written as follows:

$$\left. \begin{aligned} i_{21}(\psi, \psi_1) &= 3/4 \left\{ \frac{1}{(1 - 2/3 \cos \psi_1)^3} - 1 \right\} - \frac{9(1 - 2/3 \cos \psi_1)}{16} \left\{ \frac{1}{(1 - 2/3 \cos \psi_1)^4} - 1 \right\} \\ i_{22}(\psi, \psi_1) &= 3/8 \left\{ \frac{1}{(1 - 2/3 \cos \psi_1)^4} - 1 \right\} \end{aligned} \right\} \quad (27)$$

These equations apply to the case for which  $\psi > \psi_1$ , if  $\psi < \psi_1$  the quantity  $\psi_1$  in the above expressions for the influence functions has to be substituted by  $\psi$ .

The summation in Equation (24) has to be taken over all Multhopp stations on one half of the wing ( $n = 13$ ).

For the sake of completeness the vertical wing displacements are derived from the first Equation in (17). To get an insight into the degree of deformation, wing deflections were calculated only at the tip (for which  $i = 13$ ) from:

$$Z_{tip} = Z_{i=13}$$

$$= \frac{\pi}{192} \frac{qb^5}{B_0 \cos^4 \theta} \sum_{j=1}^n (i_{11})_{ij} \gamma_j - \frac{\pi}{96} \frac{qb^4 c_0 \tan \theta}{B_0 \cos^2 \theta} \sum_{j=1}^n (i_{12})_{ij} \mu_j \quad (28)$$

## 6. CALCULATION OF THE DOWNWASH OF THE ELASTIC WING AT THE HORIZONTAL TAIL

Because the superposition method is based on the superposition of a number of quantities corresponding with different angle-of-attack distributions, it will be

necessary to calculate the downwash caused by each selected basic load condition (angle-of-attack distribution) in order to be able to determine the resulting downwash at the horizontal tail. The station for which the downwash was determined is located at an equal distance from the plane of symmetry as the first pivotal (Multhopp) point on the wing. This location produces, according to practice, a representative value of the average downwash at the horizontal tail (roughly 1/6 of the tailspan out of the centre), so that the computational work can be limited to this station. The downwash at this point due to a given  $\alpha$ -distribution may be considered to consist of 4 parts:

$$\epsilon = \epsilon_1 + \epsilon_2 + \epsilon_3 + \epsilon_4 \quad (29)$$

The components  $\epsilon_1$  and  $\epsilon_2$  are due to the bound vortices of the right and left wings respectively, while  $\epsilon_3$  and  $\epsilon_4$  originate from the trailing vortices of the right and left wings respectively.

The 4 quantities  $\epsilon_1 \dots \epsilon_4$  are calculated with the help of the following formula for the induced normal velocity  $w$  in a point at a distance  $r$  from a vortex-line with circulation  $\Gamma$ :

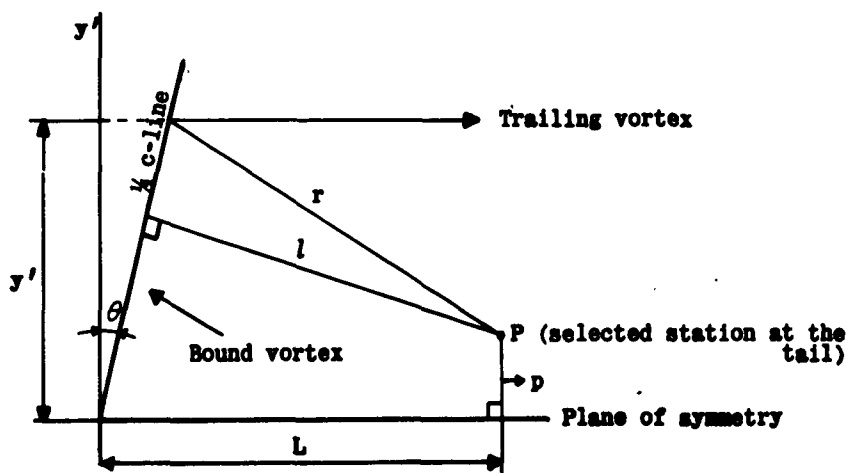
$$dw = \frac{\Gamma ds \cos \alpha}{4 \pi r^2} = \frac{\Gamma \cos \alpha}{4 \pi l} d\alpha \quad (30)$$

where  $\alpha$  is the angle between  $r$  and the normal  $l$  on the vortex line.

Integration of Equation (30) yields formulae for the components  $\epsilon_1$ .

For the downwash angle  $\epsilon_1$  induced by the bound vortex of the half wing located at the same side of the plane of symmetry as the chosen tail station P the following relation was derived:

$$\epsilon_1 = \frac{b^2 l \cos^2 \theta}{8 \pi} \frac{\pi}{24} \sum_{i=1}^n \frac{\gamma_i \sin \psi_i}{\sqrt{([\frac{1}{2} b \cos \psi_i - (l \sin \theta + p)]^2 + l^2 \cos^2 \theta)^{3/2}}} \quad (31)$$



The symbols  $l$  and  $p$  are defined in the sketch herewith. The distance of the station  $P$  from the bound vortex at the quarter-chord line of the wing is denoted by  $l$ , while the distance of this point  $P$  to the plane of symmetry is equal to  $p$ .

The downwash angle  $\epsilon_2$  induced by the bound vortex on the half wing at the other side of the plane of symmetry may be expressed by:

$$\epsilon_2 = \frac{b^2 l' \cos^2 \theta}{8\pi} \frac{\pi}{24} \sum_{i=1}^n \frac{\gamma_i \sin \psi_i}{\sqrt{\left(\left(\frac{1}{2} b \cos \psi_i - (l' \sin \theta - p)\right)^2 + l'^2 \cos^2 \theta\right)^{3/2}} \quad (32)$$

Evidently the quantity  $l'$  represents the distance of  $P$  to the quarter-chord line of the other half wing.

In the sketch an arbitrary trailing vortex is drawn.

The relation for the downwash angle  $\epsilon_3$  induced at the point  $P$  by the trailing vortices at the right hand side of the plane of symmetry reads:

$$\epsilon_3 = \frac{b}{96} \sum_1^n \left( \frac{\partial \gamma}{\partial y'} \right)_1 \left\{ 1 + \frac{L - \frac{b}{2} \cos \psi_1 \tan \theta}{\sqrt{\left(\frac{b^2}{4} \frac{\cos^2 \psi_1}{\cos^2 \theta} - l \cos \psi_1 (L \tan \theta + p) + p^2 + L^2\right)}} \right\} - 2 \left( \frac{\partial \gamma}{\partial y'} \right)_{y'=p} \left[ \frac{\frac{b}{2} \sin \psi_1}{\frac{b}{2} \cos \psi_1 - p} + \frac{b}{2\pi} \left( \frac{\partial \gamma}{\partial y'} \right)_{y'=p} \ln \left( \frac{b}{2p} - 1 \right) \right] \quad (33)$$

The differential quotient  $\partial \gamma / \partial y'$  can be derived directly from the Multhopp computations ( $\partial \gamma / \partial y' = \frac{1}{2} b \partial \gamma / \partial \eta$ ).

The downwash angle  $\epsilon_4$  induced by the trailing vortices at the other side of the wing can be written:

$$\epsilon_4 = \frac{b}{96} \sum_1^n \left( \frac{\partial \gamma}{\partial y'} \right)_1 \left\{ 1 + \frac{L - \frac{b}{2} \cos \psi_1 \tan \theta}{\sqrt{\left(\frac{b^2}{4} \frac{\cos^2 \psi_1}{\cos^2 \theta} + b \cos \psi_1 (p - L \tan \theta) + p^2 + L^2\right)}} \right\} \times \frac{\frac{b}{2} \sin \psi_1}{\frac{b}{2} \cos \psi_1 + p} \quad (34)$$

The summation  $\sum_1^n$  is carried out over the Multhopp pivotal points selected before.

For each of the selected angle-of-attack distributions one value of  $\epsilon = (\epsilon_1 + \epsilon_2 + \epsilon_3 + \epsilon_4)$  is computed. It is possible now to determine a final value

of the downwash gradient with the superposition method starting from a chosen initial condition.

The following aircraft dimensions have been used for the numerical evaluation of the downwash formulae:

$$L = 19 \text{ m}$$

$$b = 36 \text{ m}$$

$$\theta = 32.5^\circ$$

$$p = 2.35 \text{ m} \left( = \frac{b}{2} \sin \frac{\pi}{24} \right)$$

### 7. FUSELAGE BENDING

In addition to the aeroelastic deformation of the wing, fuselage-bending has also been taken into account. For this purpose use was made of the approximative method given in Reference 5, in which a relation is derived between the lift-gradients of the horizontal tailplane with and without the effects of elastic deformation of the fuselage:

$$A_t = \frac{A_{tR}}{1 + A_{tR} J q} \quad (35)$$

Here  $A_t$  and  $A_{tR}$  represent the lift gradients of the horizontal tail with and without the influence of fuselage bending. The quantity  $J$  can be roughly estimated with the help of the following relation:

$$J = 0.715 \frac{S_t l^2}{(EI_f)_0} \quad (36)$$

in which it has been assumed that the bending stiffness of the fuselage varies according to:

$$\begin{aligned} (EI_f)_x &= (EI_f)_0 \left( \frac{h_x}{h_0} \right)^3 \\ &= (EI_f)_0 \left( 1 - \frac{1}{2} \frac{x^2}{l_t^2} \right)^3 \end{aligned} \quad (37)$$

The X-axis in this case was supposed to coincide with the axis of symmetry of the fuselage. The length of the fuselage  $l_t$  ( $= 16.5\text{m}$ ) is taken from the origin of the X-axis, where the fuselage is assumed to be clamped (roughly at the quarter-chord point of the wing midchord). The height of the fuselage varies parabolically.

The numerical value of the quantity  $J$  is  $8.65 \times 10^{-6} \text{ kg}^{-1} \text{ m}^2$ , based on the following estimation of the bending stiffness:

$$(EI_f)_0 = 6 \times 10^9 \text{ kgm}^2$$

With these data the lift gradient  $A_t$  can now be calculated for each Mach number.

### 8. THE 'EXACT' METHOD TO CALCULATE THE DISTRIBUTION OF THE AERODYNAMIC LOADING OF AN ELASTIC WING

In the preceding sections it was mentioned that in order to check the results of the superposition method a second method has been applied to calculate the load distribution on the elastic wing more exactly.

This method is based on the solution of a number of linear equations with the dimensionless lift- and pitching-moment coefficients  $\gamma$  and  $\mu$  as unknowns. The coefficients of  $\gamma$  and  $\mu$  in these equations are obtained by using the following fundamental equation:

$$\alpha_P(\eta_i) = \alpha_I(\eta_i) + \alpha_E(\eta_i) \quad (38)$$

In this equation the angle-of-attack distribution  $\alpha_E(\eta_i)$  is a linear polynomial of  $\gamma$  and  $\mu$ . The final load distribution on the elastic wing is determined by the final angle-of-attack distribution  $\alpha_P$ , by means of the Multhopp equations for  $\mu$  and  $\gamma$ , which can be written for a wing with a symmetrical cross-section as follows:

$$\gamma_i = a_{11}(l_i' - l_i^n) \alpha_{P_1} + \sum_{j=1}^{n_{1i}} B_{1j} \gamma_j + \sum_{j=1}^{n_{1i}} C_{1j} \mu_j \quad (39)$$

In the same way an expression is obtained for  $\mu$ :

$$\mu_i = a_{11}(m_i^n - m_i') \alpha_{P_1} + \sum_{j=1}^{n_{1i}} D_{1j} \gamma_j + \sum_{j=1}^{n_{1i}} E_{1j} \mu_j \quad (40)$$

The subscripts on the summation symbol are introduced to denote that  $i \neq j$ . All coefficients occurring in Equations (39) and (40) can be calculated from special tables given by Multhopp, when the geometry of the wing is known. Subsequently the final angle-of-attack distribution  $\alpha_P$  is substituted according to Equation (38) by the initial and the elastic angle-of-attack distributions. For the  $\alpha_E$ -distribution the expression from Equation (24) can be substituted, while the  $\alpha_I$ -distribution is a known function of the spanwise co-ordinate. (In this investigation  $\alpha_I$  is constant along the span). After carrying out the above mentioned substitutions there appear a number of equations which are linear in  $\mu$  and  $\gamma$ . Solution of these equations yields the final distributions of lift and pitching moment.

Although the principles of this method are relatively simple, the introduction of compressibility when considering different air speeds produces a considerable quantity of additional computational work.

#### 9. COMPARISON OF THE RESULTS OF WING LOAD CALCULATIONS WITH THE SUPERPOSITION METHOD AND THE 'EXACT' METHOD

The results of the lift computations obtained with the 'exact' method were used as a measure for the reliability of the superposition method, dealt with in Section 3.2.

The most important influence of the differences between the results of both methods is due to the way in which compressibility is taken into account. The superposition method is based on the assumption that the shape of the load distribution does not change with increasing Mach number. One of the consequences of this assumption is that the centre of pressure of the section does not shift. The exact method applies transformed equations for the computation of lift and pitching moment according to the 'Prandtl-Glauert' rule when compressibility is taken into account. The effect of this transformation, the so-called 'co-ordinate-reduction', is a change of shape in the lift distribution, especially along the wing chord, so that movements of the centre of pressure occur.

The comparison between the two methods was carried out for a Mach number of  $M = 0.8$  (sub-critical) in order to obtain the largest possible difference between the results. As a matter of fact this Mach number is relatively high as far as the validity of the 'Prandtl-Glauert' rule is concerned.

In Figure 1 load distributions are given for an altitude of 10,000 m, expressed by the product  $2b\gamma = C_l c$  as a function of the spanwise co-ordinate ( $\eta$ ). Integration of this product over the span yields:

$$\int_0^A C_l c \, d\eta = C_{L_w} \left( \frac{S}{b} \right) \quad (41)$$

Since the calculations discussed here start from an angle of attack of 1 radian the lift coefficient  $C_{L_w}$  obtained with Equation (41) is in fact a lift gradient  $A$ .

Two curves have been drawn in Figure 1 for the rigid wing. One of these load distributions (full line) was obtained by multiplying the corresponding results computed for incompressible flow with the factor  $P$  earlier mentioned (Eqn.13), whereas the second one (dotted line) was determined directly for the required Mach number according to Multhopp's method.

The load distributions calculated for the aeroelastically deformed wing calculated with the superposition method (full line) and the 'exact' method (dotted line) are given by the two lower curves. The difference between the results of both methods appears to be very small and may be practically neglected, notwithstanding the fact that the superposition method is based on a very rough estimation of the compressibility effects compared with the exact method (see Section 3.2).

Further information referring to the reliability of the superposition method may be obtained by comparing the lift gradients computed from the load distributions with Equation (41). According to the exact method the lift gradient  $A$  changes from 5.51 for the rigid wing to 4.73 in the deformed condition. The corresponding figures for the superposition method are 5.43 and 4.71. On account of these results it appears that the applicability of the superposition method is permissible.

In a similar way the corresponding curves for the distributions of the pitching moment (expressed as  $2b\mu$ ) were computed and these are drawn in Figure 2. As a consequence of the way in which compressibility has been taken into account the two curves of the pitching-moment distribution for the rigid wing show remarkable differences. However, to appreciate the influence of aeroelasticity on the longitudinal stability of aircraft, it is the total shift of the centre of pressure, being identical to the aerodynamic centre for the wing with symmetrical cross-section under consideration, which is of primary importance, not its absolute location. Comparing now the shifts of the centre of pressure according to both methods, the following results may be enlightening.

According to the 'exact' method the location of the centre of pressure for the rigid condition is at  $-1.53 \bar{c}$  (that is behind the apex of the wing); this shifts to  $-1.49 \bar{c}$  for the elastic wing under the same conditions. Calculations according to the superposition method produce a shift from  $-1.49 \bar{c}$  to  $-1.45 \bar{c}$ . In both cases a forward shift is found of  $4\% \bar{c}$ . From this point of view also the applicability of the superposition method is justified.

To judge the mutual differences between both methods, the elastic angle-of-attack distribution ( $\alpha_{E_1}$ ) has been considered. The results are given in Figure 3. The total elastic angle of attack was computed according to the superposition method using the following relation:

$$\alpha_{E_1} = A_s \alpha_{E_1_1} + B_s \alpha_{E_1_2} + C_s \alpha_{E_1_3} + \alpha'_{E_1} \quad (42)$$

In this equation the quantities  $\alpha_{E_1(1,2,3)}$  and  $\alpha'_{E_1}$  represent the changes of the angle-of-attack distributions due to aeroelastic deformation at the 'Muthopp' stations on the wing caused by the loadings following from the final distributions  $\alpha_p = \eta, \eta_1^2, \eta^3$  and 1 radian.

The component curves (dotted lines) of the resultant  $\alpha_{E_1}$  (small circles) are also drawn in Figure 3 in agreement with Equation (42). To get an insight into the accuracy of the approximation of the elastic angle-of-attack distributions  $\alpha_E$  by a third-degree function in  $\eta$  (determination of the coefficients  $a_1, b_1,$  and  $c_1$ ), the resultant  $\alpha_E$  was computed moreover from:

$$\alpha_E = A_s \eta + B_s \eta^2 + C_s \eta^3 \quad (43)$$

The  $\alpha_E$ -curve is given by the full line in Figure 3. It appears from the location of the small circles (Equ. (42)) with regard to this full-line curve (Equ. (43)) that the approximation is fully justified as both computations lead to the same result.

Finally, the elastic angle-of-attack distribution according to the exact method was calculated by substituting the corresponding values of  $\gamma$  and  $\mu$  into Equation (39). The distribution  $\alpha_F$  is now solved and the distribution  $\alpha_E$  follows from:

$$\alpha_{E_1} = \alpha_{F_1} - \alpha_{I_1} \quad (44)$$

The values  $\alpha_{E_1}$  computed in this way are inserted into Figure 3 as separate data. Comparing now the results of the two methods under consideration it appears from Figure 3 that the differences are only small. In the most unfavourable case they only amount to about 10% of the total change. It may be concluded from the above results that no predominant objections against the application of the superposition method are present. Consequently, the remaining part of the investigation has been carried out according to this method.

## 10. INVESTIGATION OF THE INFLUENCE OF AEROELASTICITY ON THE STATIC LONGITUDINAL STABILITY OF AN AIRCRAFT WITH SLENDER SWEEP-BACK WINGS

### 10.1 Basic Data for the Calculation

Before passing on to the proper treatment of the problem a summary is given of the numerical values of the quantities which have served as a basis for the calculations:

|  |   |
|--|---|
| $W = 100,000 \text{ kg}$                               | $B_0 = 10^9 \text{ kgm}^2$  |
| $S = 162 \text{ m}^2$                                  | $T_0 = 0.25 \times 10^8 \text{ kgm}^2$                                    |
| $b = 36 \text{ m}$                                     | $S_t = 25 \text{ m}^2$  |
| $\lambda = 8$ (aspect ratio)                           | $b_t = 10 \text{ m}$  |
| taper ratio 1/3  | $l_t = 16.5 \text{ m}$ (distance of c.g. to a.c. of horizontal tailplane) |
| $c_0 = 6.75 \text{ m}$ (root chord)                    | $(At_r)_{M=0} = 3.65$   |
| $\theta = 31.5^\circ$ (angle of sweep of elastic axis) | $v_t = 0.565$   |

Table I gives the flight conditions for which the deformations have been calculated.

The centre of gravity was assumed to be located at  $0.1 \bar{c}$  behind the aerodynamic centre of the rigid wing, that is  $1.595 \bar{c}$  behind the apex of the swept wing. The quantity  $(x_{c.g.} - x_{a.c.})$ , which occurs in the pitching-moment equation for the equilibrium condition, is for the compressible as well as for the incompressible flow equal to  $0.1 \bar{c}$  (the superposition method supposes that the load distribution along the wing chord does not change shape with increasing Mach number). With the help of the superposition method the final distributions of  $\gamma$  and  $\mu$  were calculated. From these the pitching moment coefficient (with reference to the normal on the plane of symmetry in the apex of the wing) and the lift coefficient were derived. The

location of the wing centre of pressure ( $x_{c.p.} = x_{a.c.}$ ) was derived from the ratio  $C_M/C_L$ . The numerical values  $(x_{c.g.} - x_{c.p.})/\bar{c}$  are given in Table II.

The downwash angle at the horizontal tail also has been determined by the superposition method. The values  $d\epsilon/d\alpha$  are summarized in Tables IIIa and IIIb.

Finally, a fuselage pitching-moment coefficient has been assumed, viz.  $C_{M_f} = -0.015$ ; the influence of elastic deformation was left out of consideration but the influence of compressibility was taken into account in the following way:

$$C_{M_f} = -\frac{0.015}{\sqrt{(1 - M^2)}} \quad (45)$$

## 10.2 Survey of the Calculations

As has been mentioned already when defining the problem, a hypothetical aircraft has been considered consisting of an elastic swept-back wing, an elastic fuselage and a rigid all-movable tailplane.

Because stability margins have no practical meaning at high speed, only elevator angles to trim have been calculated for the steady rectilinear flight, whereas manoeuvre margins and elevator deflections per 'g' have been computed for the steady accelerated flight.

In order to get an insight into the separate influences of aeroelasticity and compressibility, the calculations were carried out for the cases listed in Table IV, for two flight altitudes.

## 10.3 Results

The elevator deflections in steady flight have been determined from the pitching moment equation for the equilibrium condition. Remembering that  $x_{c.p.} = x_{a.c.}$ , this equation is, for the aircraft with an all-movable tailplane,

$$\begin{aligned} C_M &= 0 \\ &= C_{M_f} + \frac{x_{c.g.} - x_{c.p.}}{\bar{c}} C_L - v_t \left\{ \frac{A_t}{A} \left( 1 - \frac{d\epsilon}{d\alpha} \right) C_L + A_t \delta_t \right\} \end{aligned} \quad (46)$$

In this equation the tail volume  $v_t$  follows from:

$$v_t = \frac{v_{c.p.}}{1 + \frac{A_t}{A} \frac{S_t}{S} \left( 1 - \frac{d\epsilon}{d\alpha} \right)} \quad (47)$$

in which

$$v_{c.p.} = c_{c.g.} + \frac{x_{c.g.} - x_{c.p.}}{\bar{c}} \quad (48)$$

The manoeuvre margin may be written as follows:

$$H_m = \frac{x_{c.p.} - x_{c.g.}}{\bar{c}} + A_t v_t \left\{ \frac{1}{A} \left( 1 - \frac{d\epsilon}{d\alpha} \right) + \frac{1}{2\mu} \right\} \quad (49)$$

and the elevator deflection per 'g' may be calculated from:

$$\delta_g = \frac{C_L}{A_t v_t} H_m \quad (50)$$

A picture of the static longitudinal stability in unaccelerated flight may be given with the help of the elevator deflections to trim as they follow from Equation (46). The change of these deflections with the lift-coefficient of the aircraft is reproduced in Figure 4 for  $C_{M_f} = 0$  and in Figure 5 for  $C_{M_f} = 0.015/\sqrt{1 - M^2}$ .

It follows from these figures that the influence of compressibility is considerably larger than that of aeroelasticity. It appears, furthermore, that the trim change in consequence of compressibility alone is almost constant for the whole  $C_L$ -range considered, while it is larger at higher altitudes. This is in agreement with the approximation that the influence of compressibility is proportional to the product of  $C_L$  and  $M^2$  (Ref.6).

To get a better insight into the magnitude of the trim change in consequence of aeroelasticity, the parameters occurring in Equation (46) which are of interest in this respect, viz.  $(x_{c.g.} - x_{c.p.})/\bar{c}$  and  $A (= \partial C_L / \partial \alpha)$ , are drawn separately as functions of  $C_L$  in Figures 6 to 8.

It may be deduced from these Figures and Equation (46) that the changes of the c.p. location and of lift gradient due to aeroelasticity counteract each other. Considering for instance in Figure 7 the change of lift gradient  $A$  when passing from the rigid-compressible case to the elastic-compressible one, a large decrease of  $A$  appears to occur, which is largest at the highest value of  $M$ . At the same time a shift in forward direction of the centre of pressure takes place. In Figure 6 a shift of about  $0.12 \bar{c}$  is seen at  $M = 0.8$ . The consequence of these counteracting effects is the small trim change occurring when changing from elastic to rigid conditions in compressible flow. The same applies however for the incompressible case, as may be also concluded from the corresponding curves.

Physically this may be explained also in the following way. As a consequence of deformation the c.p. of the wing will shift forward causing a nose-up change of pitching moment. Furthermore a considerable decrease of lift gradient takes place. To maintain a constant value of  $C_L$  an increase of angle-of-attack at the wing is required. It follows now that, because the tail angle-of-attack increases too, a nose-down pitching moment is generated.

The above-mentioned change of lift gradient and c.p. shift are numerically the most important parameters with respect to the trim changes. Of course the change of downwash angle due to aeroelasticity too plays a part in this respect, but this is only of small importance compared with the effects mentioned earlier.

Let us consider fuselage bending results in a change of tailplane lift gradient. This change is also relatively small, so that only a small positive trim change may be noticed from the curves of Figures 4 and 5, when passing from the case of a flexible wing only to that of both flexible wing and flexible fuselage.

Introduction of a zero-lift pitching moment of the fuselage ( $C_{M_f} = -0.015/\sqrt{1 - M^2}$ ) results in a parallel displacement of the trim curves (compare Fig.4 and Fig.5) for incompressible flow. An almost negligible trim change in a destabilizing sense occurs for the compressible flow condition at high speed. This effect is only noticeable for the curves referring to a flight altitude of 1000 m.

The manoeuvre margin stick-fixed ( $H_m$ ) has been calculated for the different cases considered using Equation (49) and drawn as a function of  $C_L$  (or  $M$ ) in Figure 9. Transition from the rigid-incompressible case to the rigid-compressible one results in a decrease of  $H_m$  with  $M$ . The effect of aeroelastic deformation is larger at lower altitudes at the same Mach number in consequence of the larger value of the dynamic pressure  $q$ . The influence of wing deformation appears to be only small. The manoeuvre margin decreases a small amount with increasing  $M$  for both compressible and incompressible flow. This decrease appears to be much larger, however, when the fuselage bending is considered additionally (decreasing  $A_t$ ).

The elevator deflections per 'g' ( $\delta_g$ ) as a function of  $C_L$  are computed from Equation (50) and are drawn in Figure 10 for all cases considered. The effect of compressibility alone is to cause a constant shift of  $\delta_g$  over the whole  $C_L$ -range with reference to the incompressible condition just as it has been shown already for the elevator trim curves. This shift increases with increasing altitude, which is in agreement with an approximate relation derived in Reference 6, according to which this shift should be proportional to  $C_L M^2$ .

The influence of aeroelasticity on  $\delta_g$ , however, appears to be much smaller. The combined effect of both phenomena is relatively large at low values of  $C_L$ . At  $C_L = 0.15$  (altitude 1000 m) the elevator deflection per 'g' is almost halved. This effect decreases relatively with decreasing speed.

To get an impression of the magnitude of the deformation occurring during the steady-flight conditions considered the corresponding vertical displacements of the wing tip were calculated from Equation (28) and plotted in Figure 11 together with the corresponding  $\gamma$ -distributions. It appears from this figure that the displacements of the wing-tip ( $Z_{tip}$  as a function of  $C_L$ ) are of the same order of magnitude for all values of  $C_L$ , at both altitudes. Differences occur only in the change of these displacements with  $C_L$ . The fact, however, that the wing lift for all cases considered here must be nearly equal to the aircraft weight is the reason why the range of tip displacements is only small. The bending of the wing at 10,000 m altitude decreases and at 1000 m increases with increasing  $C_L$ . This is caused by the shape of the corresponding lift distributions on the wing. At an altitude of 1000 m the lift of the wing (see Fig.11) is concentrating towards the

wing centre with increasing Mach number, so that the corresponding bending moment and consequently the tip displacement will decrease. The reverse effect occurs at 10,000 m. It appears from these calculations that considerable aeroelastic deformations may take place (vertical tip displacement of about 3.0 m) without deteriorating the longitudinal stability.

## 11. CONCLUSIONS

In order to investigate the possible variations of the longitudinal stability and control of an aircraft as affected by aeroelastic deformation (particularly of the wing), computations have been carried out for a hypothetical aircraft with slender swept-back wings. Of course the results only apply to the aircraft type considered. To be able to calculate the required basic data for this investigation, use was made of a superposition method, derived by Brown, Holtby and Martin<sup>1</sup>. With this method numerical results were obtained in a relatively rapid way for lift gradients, c.p.-locations and downwash gradients of the wing at different combinations of dynamic pressure and Mach number.

This method was checked from the point of view of accuracy by comparing the results with those of another, more exact method. For a complete application the latter requires much more computational work. The comparison has been carried out for one Mach number only ( $M = 0.8$ ).

After having shown the feasibility of the superposition method in this way the remaining basic data have been calculated according to the simplified method. With these data the characteristics of the static longitudinal stability of the aircraft have been derived, viz. elevator angles to trim, elevator angles per 'g' and manoeuvre margins stick-fixed. From these final results the following conclusions may be drawn:

- (1) When the load distributions are calculated both with the superposition method and with the 'exact method', it appears that the mutual differences of the results are sufficiently small to justify the application of the superposition method for rapid computations (Fig.1). The wing lift gradient at  $M = 0.8$  and at a dynamic pressure  $q = 1200 \text{ kg/m}^2$  changes from 5.51 to 4.73 due to aeroelasticity according to the exact method, while the figures according to the superposition method are 5.43 and 4.71 respectively.
- (2) The mutual differences of the pitching-moment distributions, however, are much larger (Fig.2). Nevertheless the derived c.p.-shifts appear to be almost equal in both cases. As only the latter is of interest for this investigation the suitability of the applied method has been proved in this respect as well. According to the exact method the wing deformation causes a shift of the c.p. from  $1.530 \bar{c}$  to  $1.490 \bar{c}$ , behind the apex of the wing, while the corresponding values according to the superposition method are 1.495 and  $1.453 \bar{c}$ . In both cases a forward shift was obtained of about  $4\% \bar{c}$ .
- (3) The deformations of the wing determined by both methods as given by the angle-of-attack distributions  $\alpha_p$  also show small mutual differences (Fig.3) for the flight conditions considered.

- (4) The longitudinal trim changes as a consequence of wing deformation of the hypothetical aircraft considered appeared to be small in compressible as well as in incompressible flow. The influence of compressibility is considerably larger (Figs.4 and 5). The effect of wing deformation on longitudinal stability results in two opposite effects, viz. a forward shift of the c.p. and a decrease of lift gradient with increasing speed, effects which almost neutralize each other.
- (5) The manoeuvre margin stick-fixed only shows an appreciable decrease, when fuselage bending is taken into account (Fig.9). The influence of compressibility, however, is much larger.
- (6) The elevator travel per 'g' undergoes a relatively large decrease as a consequence of the combined influences of compressibility and aeroelasticity, in particular, at low altitudes and high Mach numbers (Fig.10). Again the influence of compressibility is dominating.
- (7) The vertical displacements of the tip in steady flight appear to be of the order of 3.0 m; only small variations occur with changing flight conditions (see Fig.11).

Notwithstanding the considerable deformations of the wing, the changes of longitudinal stability due to aeroelasticity appear to be unexpectedly small. When comparing the above conclusion with those obtained by other investigators in this field, e.g. by Campion and Skoog<sup>4,7</sup>, similar results are given. The counteracting effects of c.p.-shift and wing-lift change due to aeroelasticity with respect to stability and trim change are particularly mentioned in both references. Likewise caution has been recommended when generalizing these results by postulating the rule that flexibility of swept-wing aircraft does not affect stability in a serious way. By a proper choice of the stiffness parameters dependent on the sweep angle of the wing it is, however, possible to avoid a too large change of the stability characteristics.

Contrary to those publications this investigation is chiefly confined to the aeroelastic deformation of the wing and fuselage bending. The weight of the aircraft wing, which generally has an alleviating effect on longitudinal stability changes, has been left out of consideration.

## REFERENCES

1. Brown, R.B.  
et alii *A Superposition Method for Calculating the Aeroelastic Behavior of Swept Wings.* Journal of the Aeronautical Sciences, August 1951.
2. Multhopp, H. *Method for Calculating the Lift Distribution of Wings. (Subsonic Lifting Surface Theory).* RAE Rep. AERO 2353.
3. Fisher, L.R. *Approximate Corrections for the Effects of Compressibility on the Subsonic Stability Derivatives of Swept Wings.* NACA Techn. Note No. 1854.
4. Campion, B.S. *Estimation of Distortion on Longitudinal Stability of Swept Wing Aircraft at High Speeds. (Sub-critical Mach numbers).* The College of Aeronautics, Cranfield Rep. No. 77.
5. Lyon, H.M.  
Ripley, J. *A General Survey of the Effects of the Fuselage Tail Unit and Control Systems on Longitudinal Stability and Control.* R. & M. 2415.
6. Buhrman, J.  
Kalkman, C.M. *The Static Longitudinal Stability and Control of an Aeroplane as Affected by the Compressibility of the Air.* NLL Report V. 1625.
7. Skoog, R.B. *An Analysis of the Effects of Aeroelasticity on Static Longitudinal Stability and Control of a Swept-Back-Wing Airplane.* NACA R.M. A 51 C 19.

TABLE I

Flight Conditions Used for Deformation Calculations  
(see Sec.10.1)

| Altitude |                       |                |                       |                |
|----------|-----------------------|----------------|-----------------------|----------------|
| M        | 10,000 m              |                | 1000 m                |                |
|          | q(kg/m <sup>2</sup> ) | C <sub>L</sub> | q(kg/m <sup>2</sup> ) | C <sub>L</sub> |
| 0.4      | -                     | -              | 1026                  | 0.601          |
| 0.6      | 682                   | 0.905          | 2309                  | 0.267          |
| 0.7      | 927                   | 0.666          | 3143                  | 0.196          |
| 0.8      | 1210                  | 0.510          | 4105                  | 0.150          |

TABLE II

Numerical Values of  $(x_{c.g.} - x_{c.p.})/\bar{c}$

| M   | Altitude |        |
|-----|----------|--------|
|     | 10,000 m | 1000 m |
| 0.4 | -        | 0.130  |
| 0.6 | 0.122    | 0.166  |
| 0.7 | 0.131    | 0.190  |
| 0.8 | 0.142    | 0.217  |

TABLE III

Values of  $dc/da$  for the Rigid and the Elastic Wing

(a) Compressible Flow

| Altitude |          |         |        |         |
|----------|----------|---------|--------|---------|
| M        | 10,000 m |         | 1000 m |         |
|          | Rigid    | Elastic | Rigid  | Elastic |
| 0.4      | -        | -       | 0.290  | 0.305   |
| 0.6      | 0.311    | 0.323   | 0.311  | 0.343   |
| 0.7      | 0.328    | 0.345   | 0.328  | 0.371   |
| 0.8      | 0.352    | 0.376   | 0.352  | 0.407   |

(b) *Incompressible Flow*

| <i>Altitude</i> |                 |                |               |                |
|-----------------|-----------------|----------------|---------------|----------------|
| <i>M</i>        | <i>10,000 m</i> |                | <i>1000 m</i> |                |
|                 | <i>Rigid</i>    | <i>Elastic</i> | <i>Rigid</i>  | <i>Elastic</i> |
| 0.4             | -               | -              | 0.276         | 0.289          |
| 0.6             | 0.276           | 0.285          | 0.276         | 0.302          |
| 0.7             | 0.276           | 0.288          | 0.276         | 0.308          |
| 0.8             | 0.276           | 0.291          | 0.276         | 0.314          |

TABLE IV

Cases Considered (see Sec. 10.2)

| <i>Incompressible Flow</i> | <i>Compressible Flow</i>   |
|----------------------------|----------------------------|
| Rigid aircraft             | Rigid aircraft             |
| Flexible wing only         | Flexible wing only         |
| Flexible wing and fuselage | Flexible wing and fuselage |

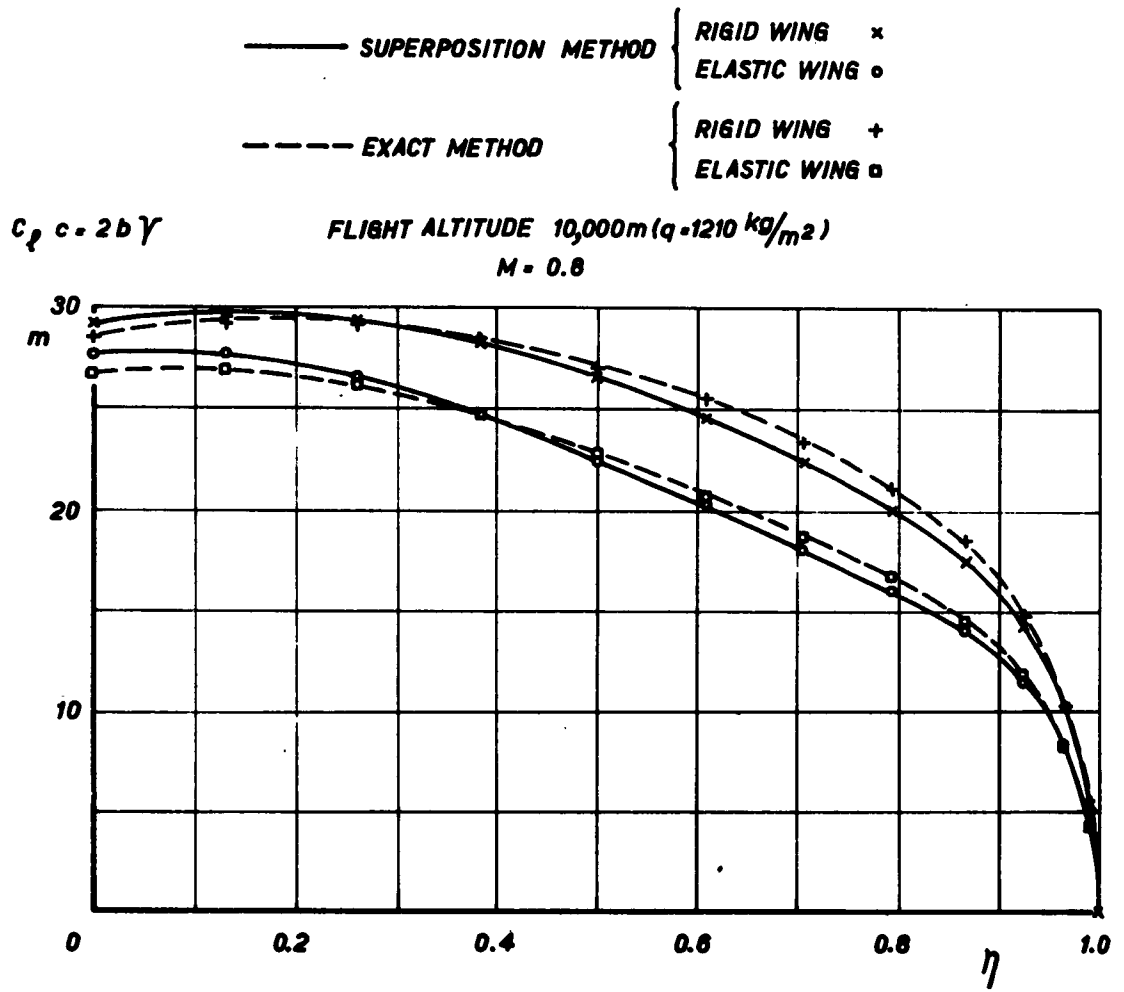


Fig.1 Load distributions for compressible and incompressible flow determined by the superposition method and by the exact method

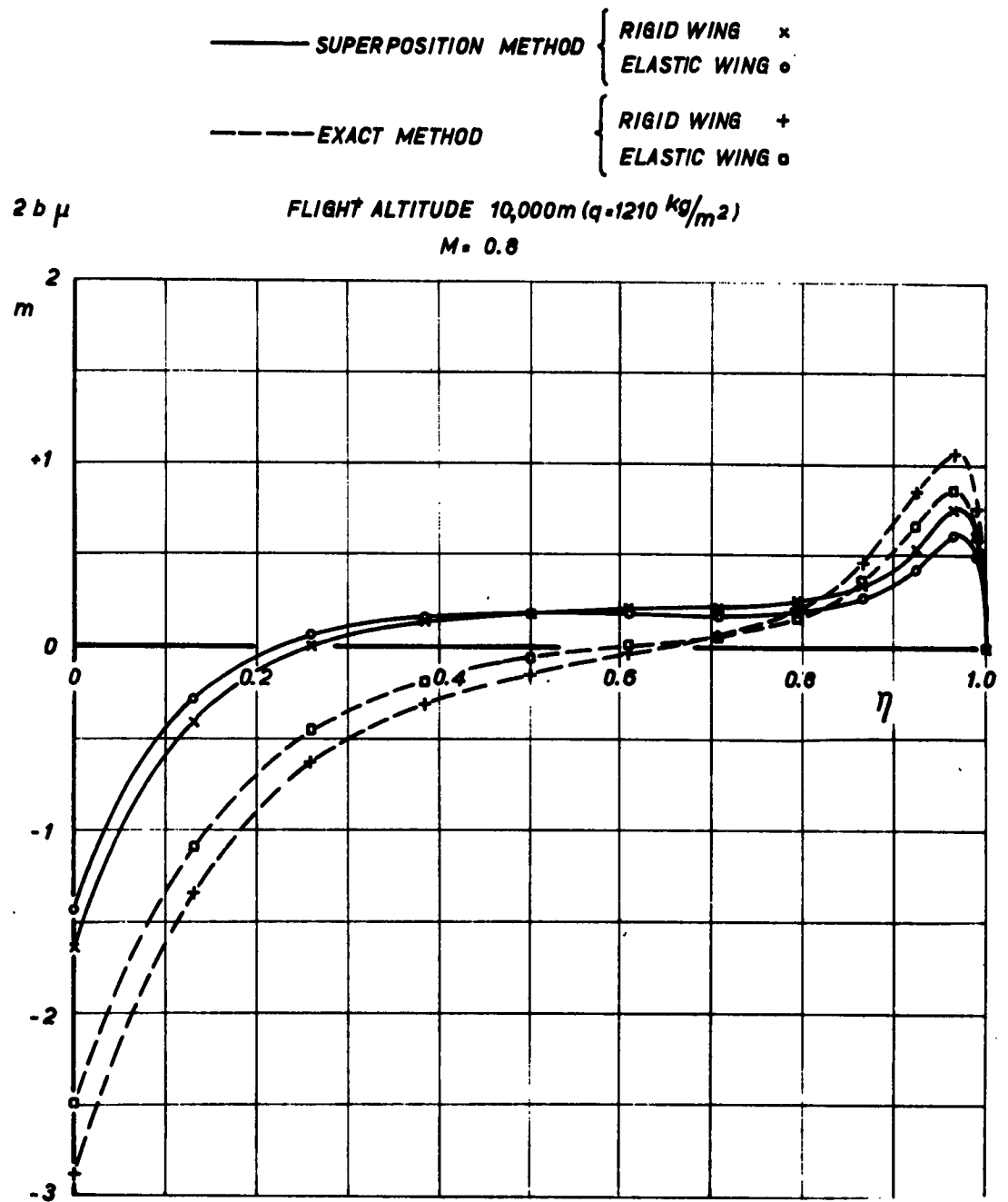


Fig. 2 Pitching moment distributions for compressible and incompressible flow determined by the superposition method and by the exact method

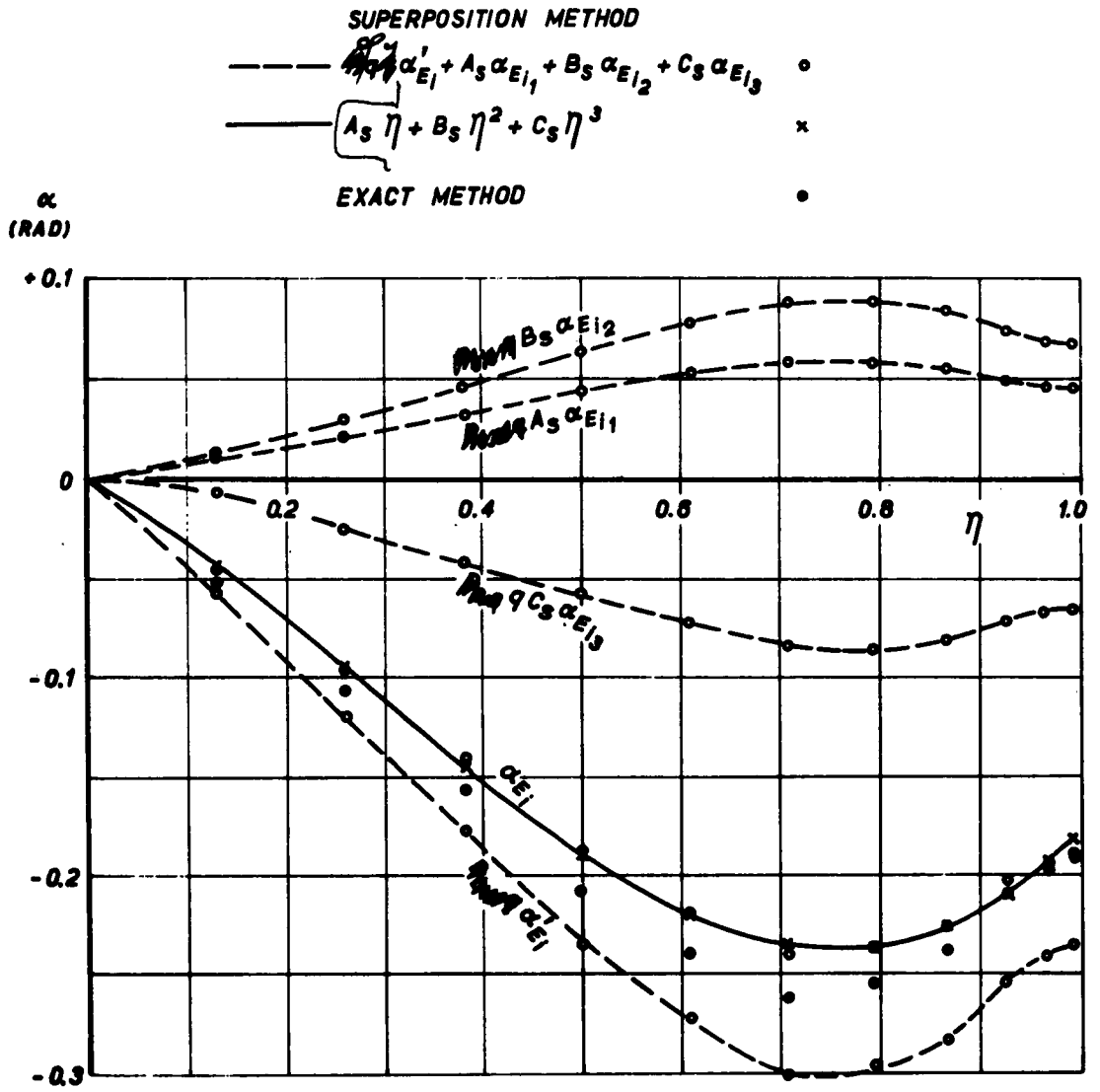


Fig.3 Superposition of angle-of-attack distributions ( $\alpha_{E1}$ ) and comparison of results with those of exact method

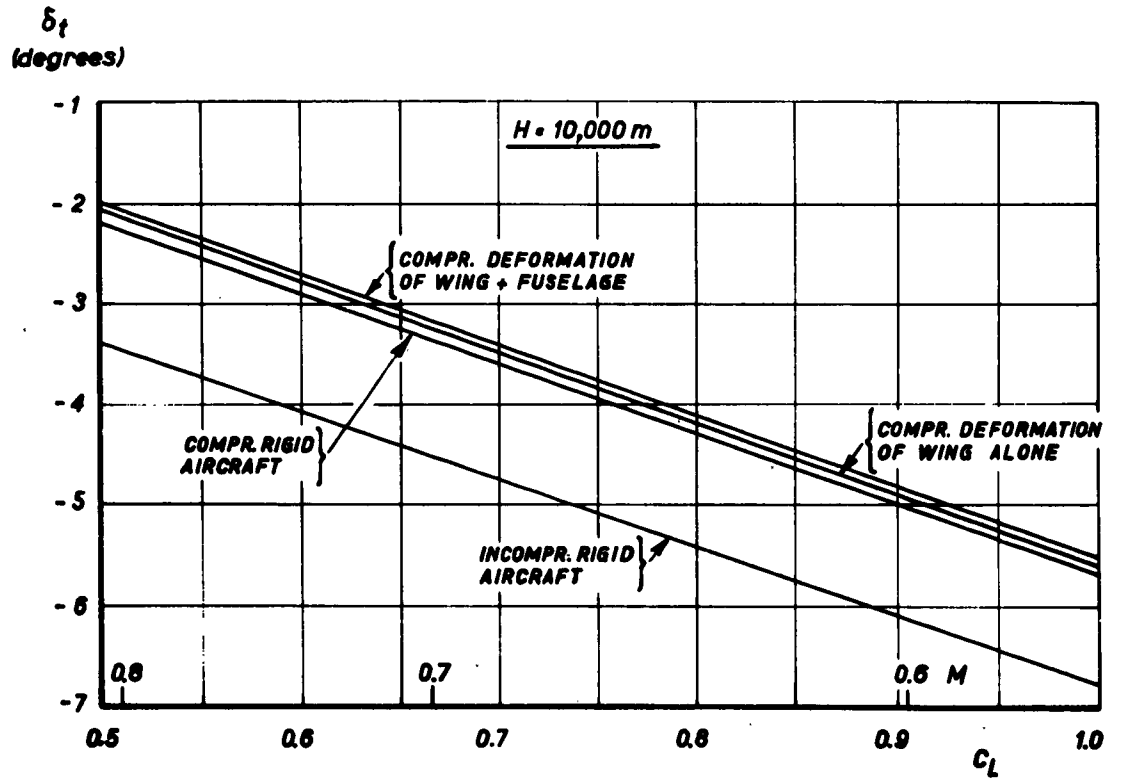
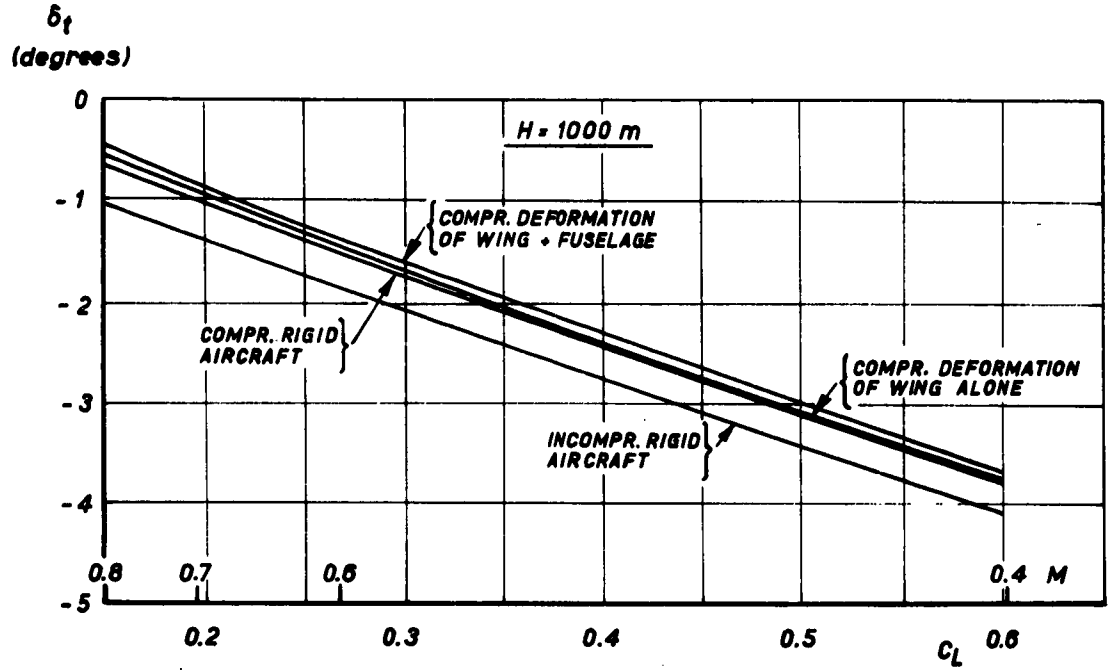


Fig. 4 Elevator deflections as a function of  $C_L$   
( $C_{M_f} = 0$ )

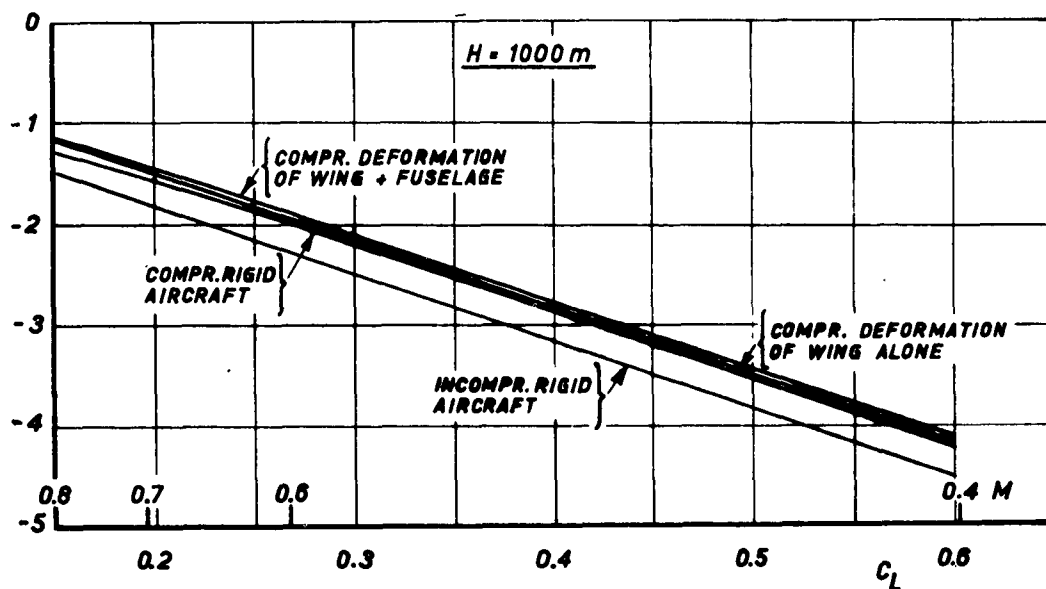
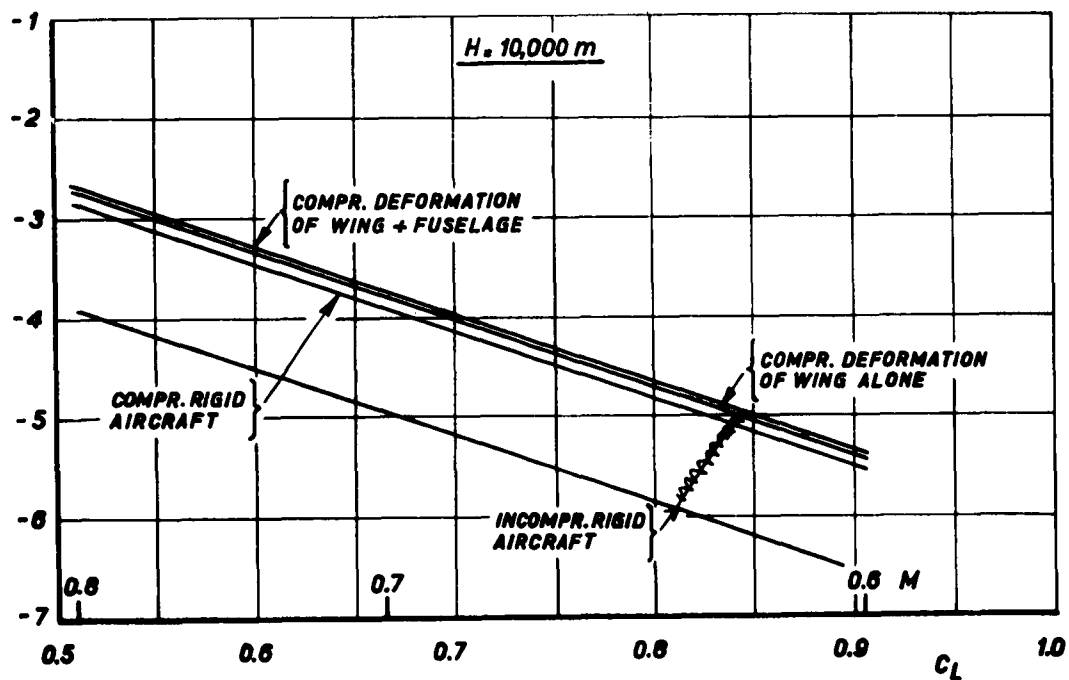
$\delta_t$   
(degrees)

 $\delta_t$   
(degrees)


Fig. 5 Elevator deflection as a function of  $C_L$   
 $(C_{M_z} = -0.015/\sqrt{1 - M^2})$

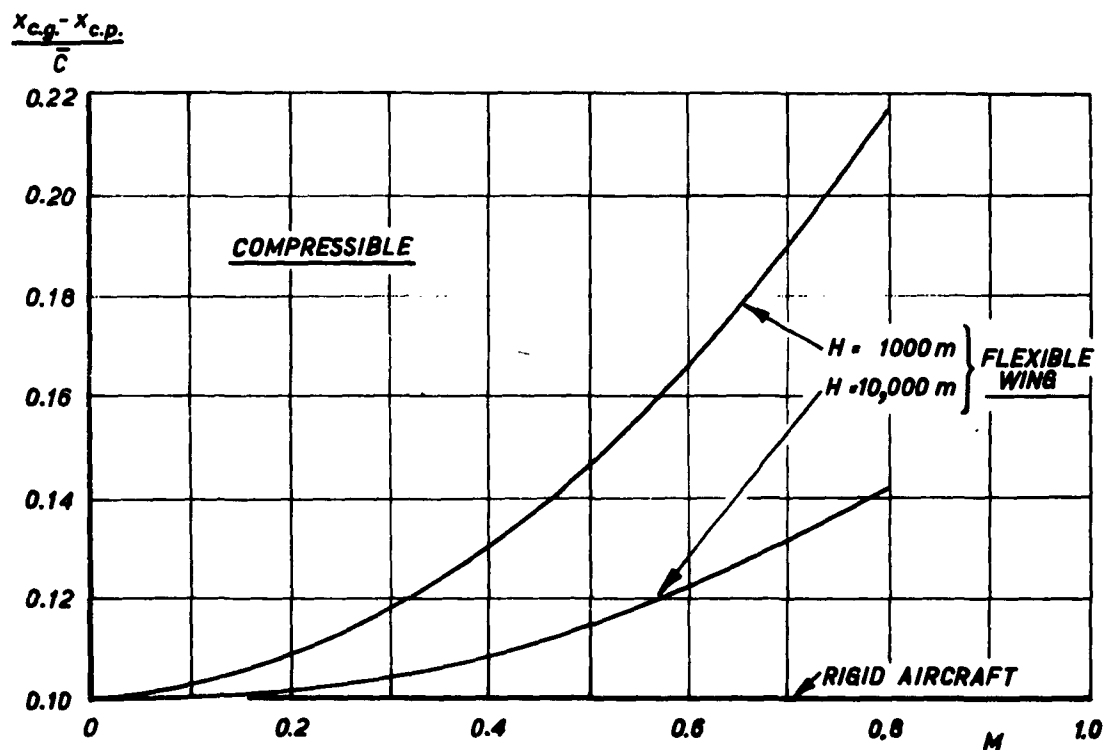
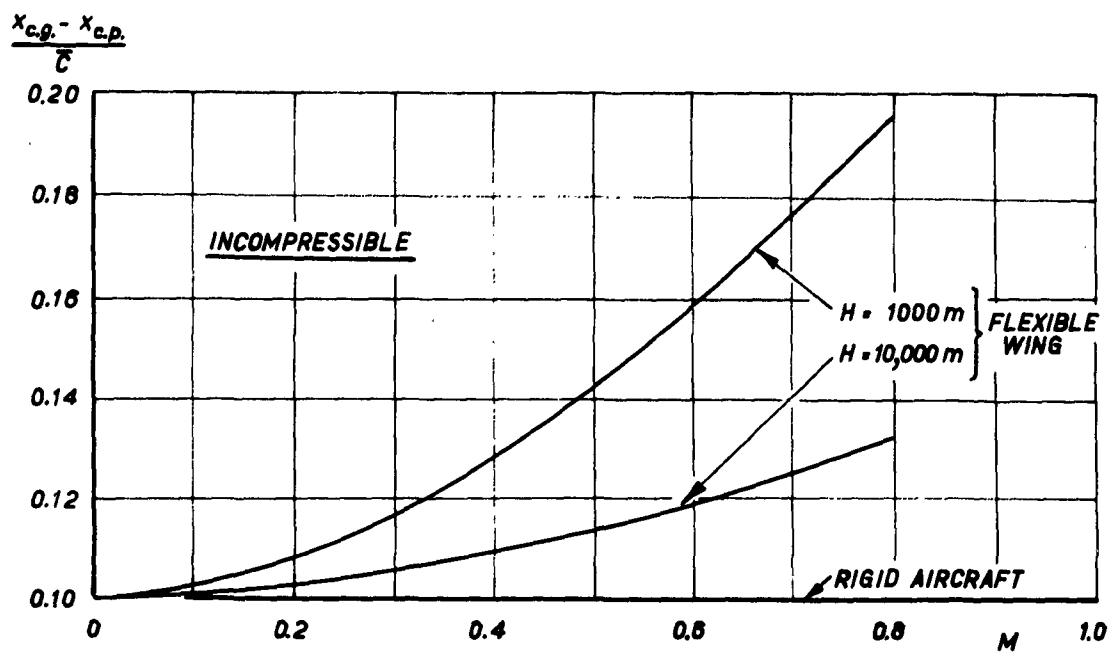


Fig. 6 Shift of centre of pressure due to aeroelasticity, with and without compressibility effects

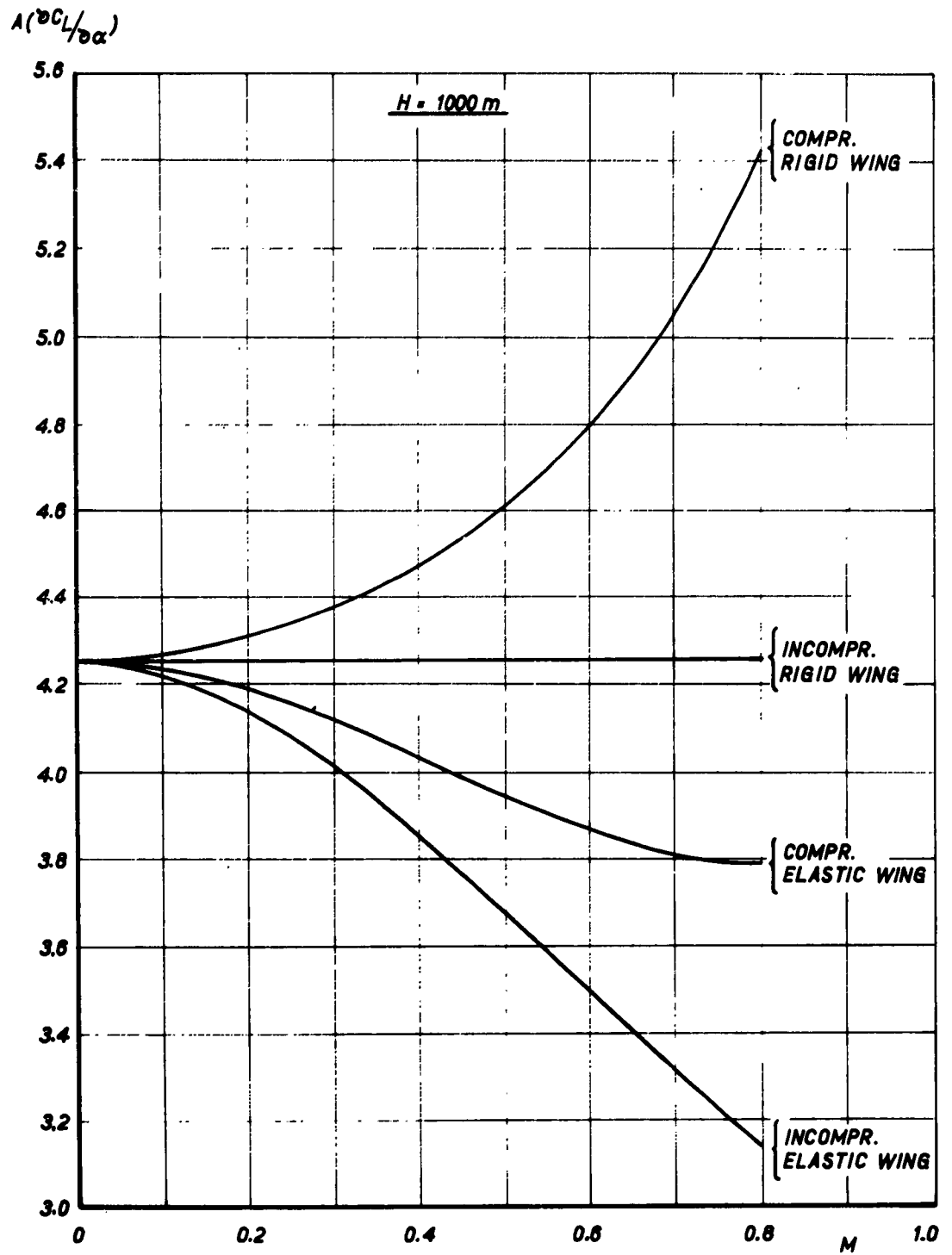


Fig. 7 Influence of compressibility and aeroelasticity on wing lift gradient

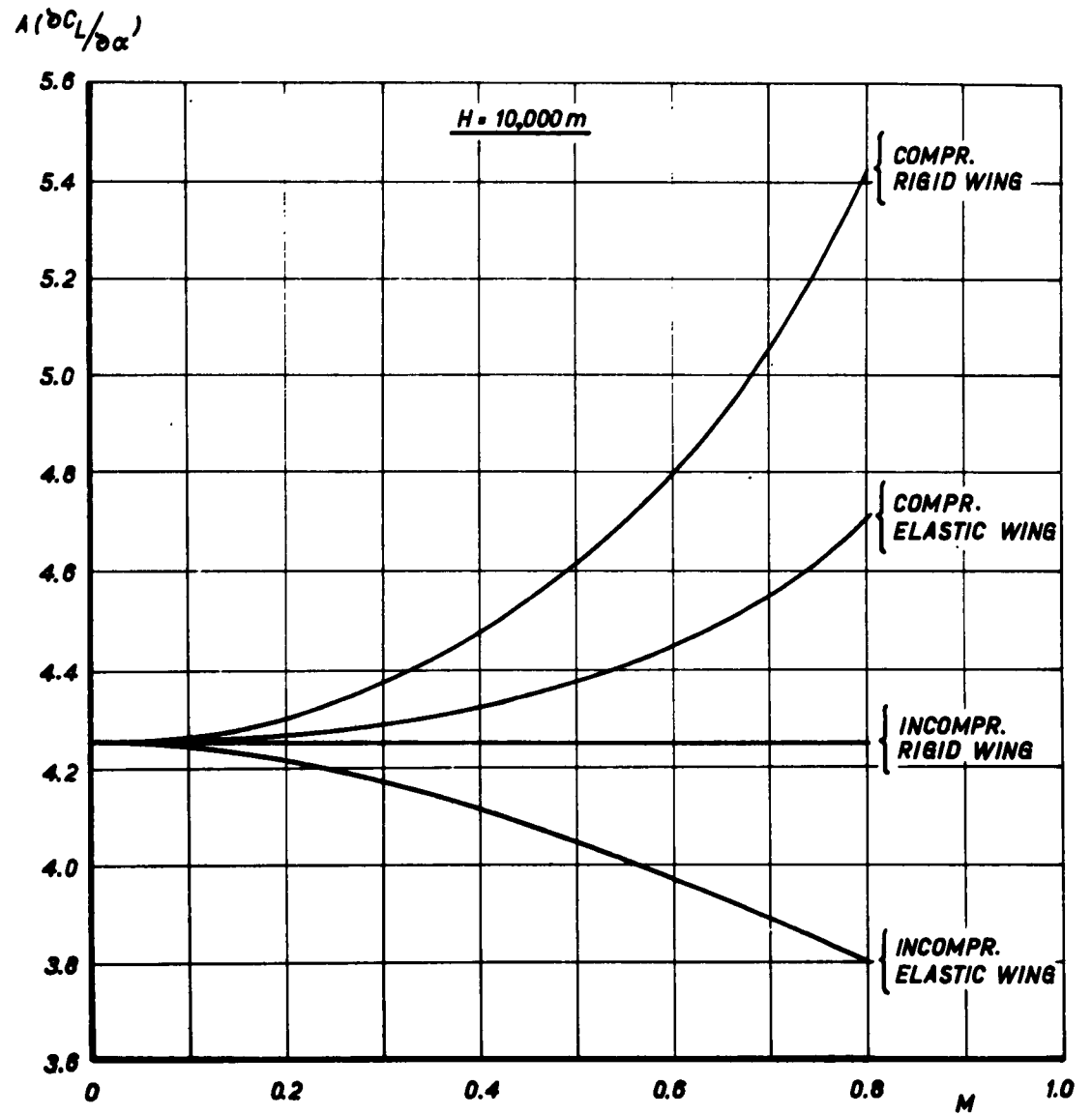


Fig. 8 Influence of compressibility and aeroelasticity on wing lift gradient

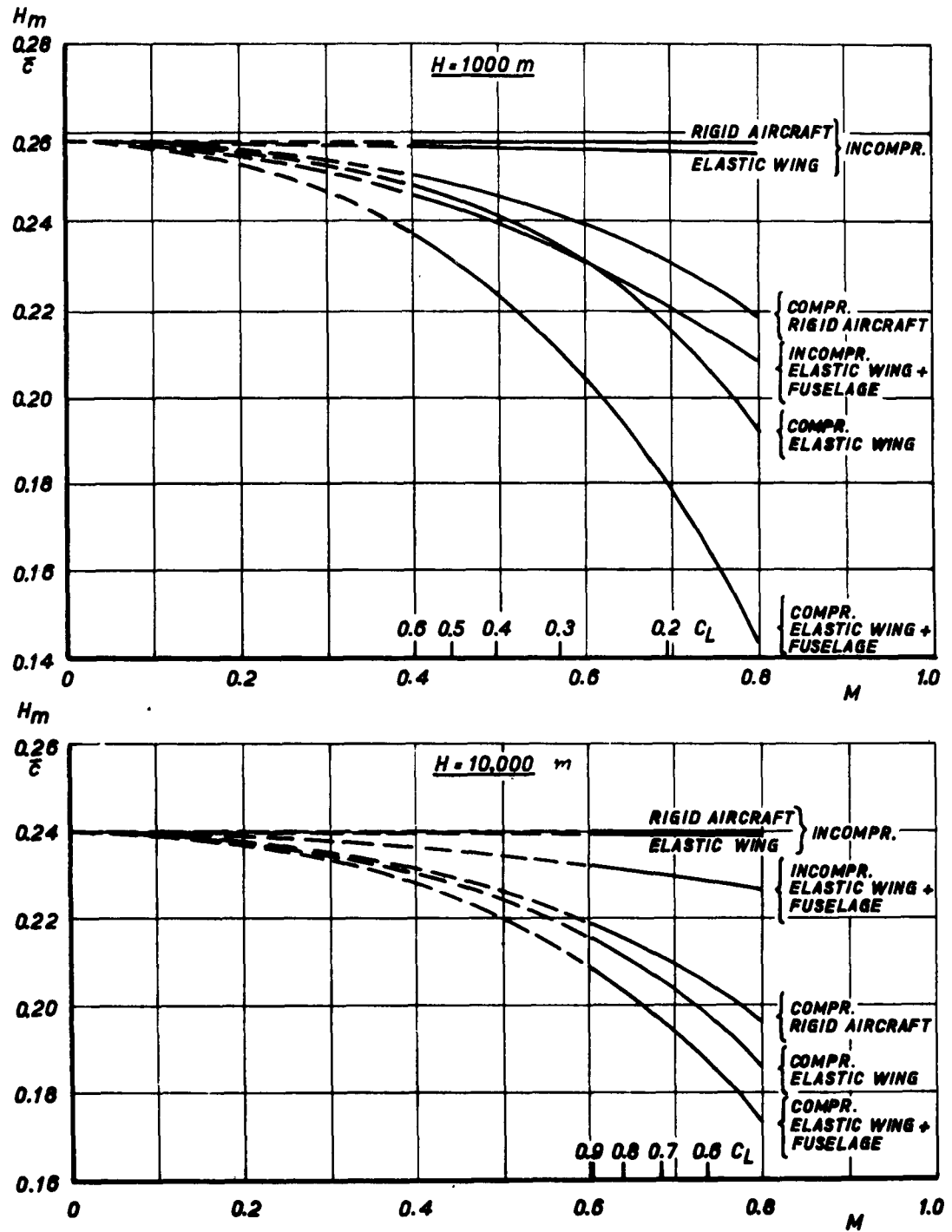


Fig. 9 Manoeuvre margins stick-fixed

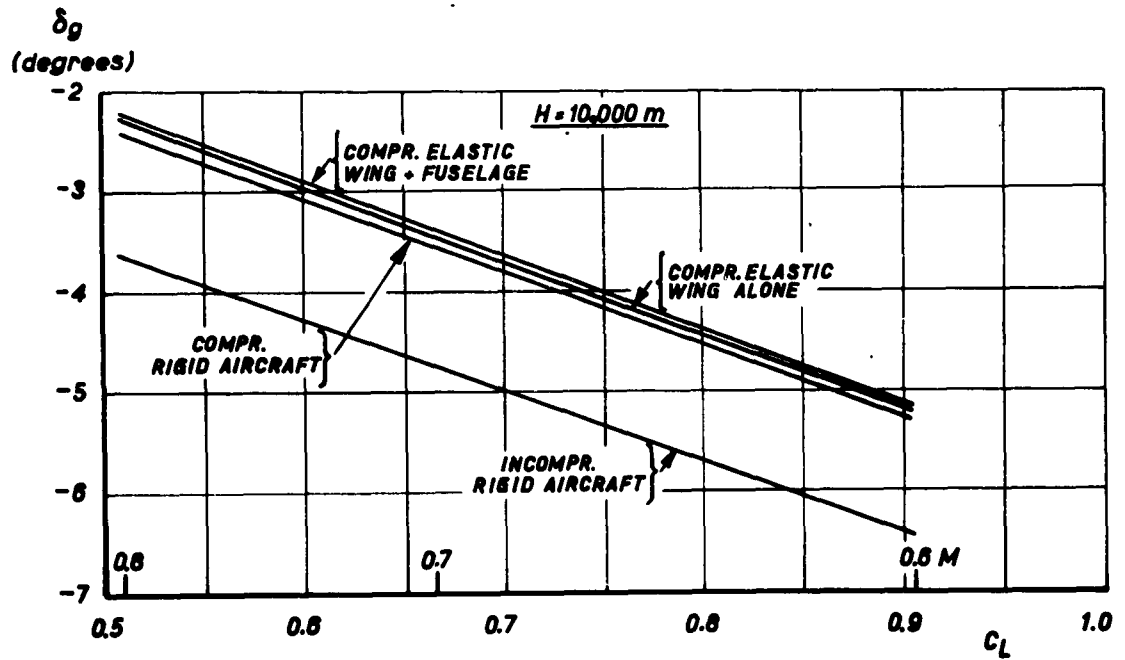
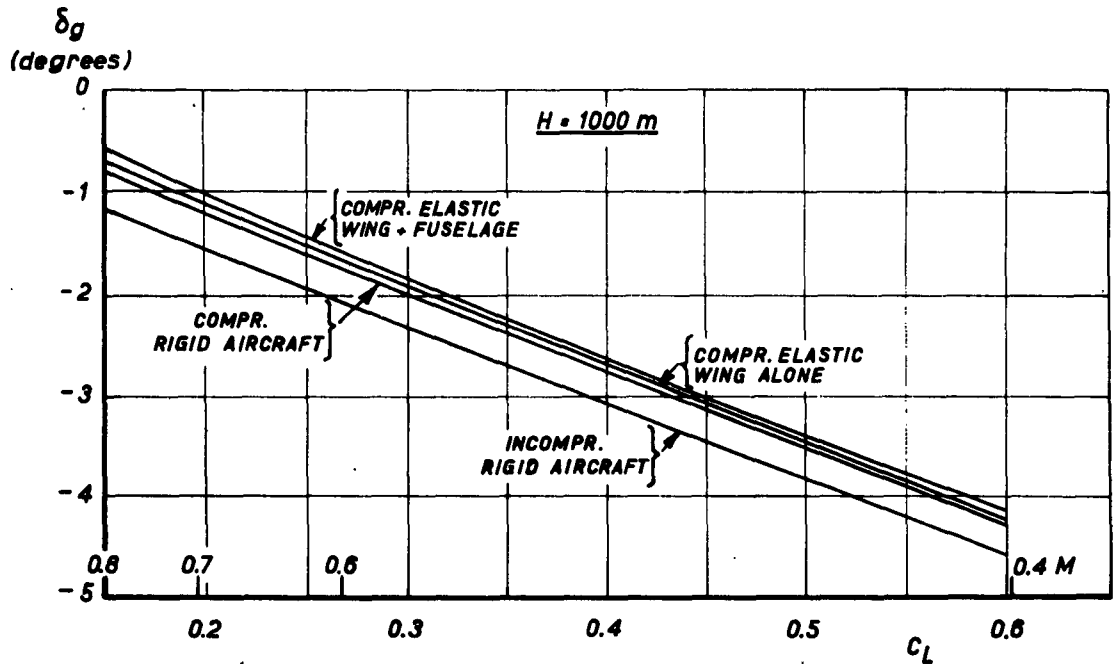


Fig. 10 Elevator travel per 'g'

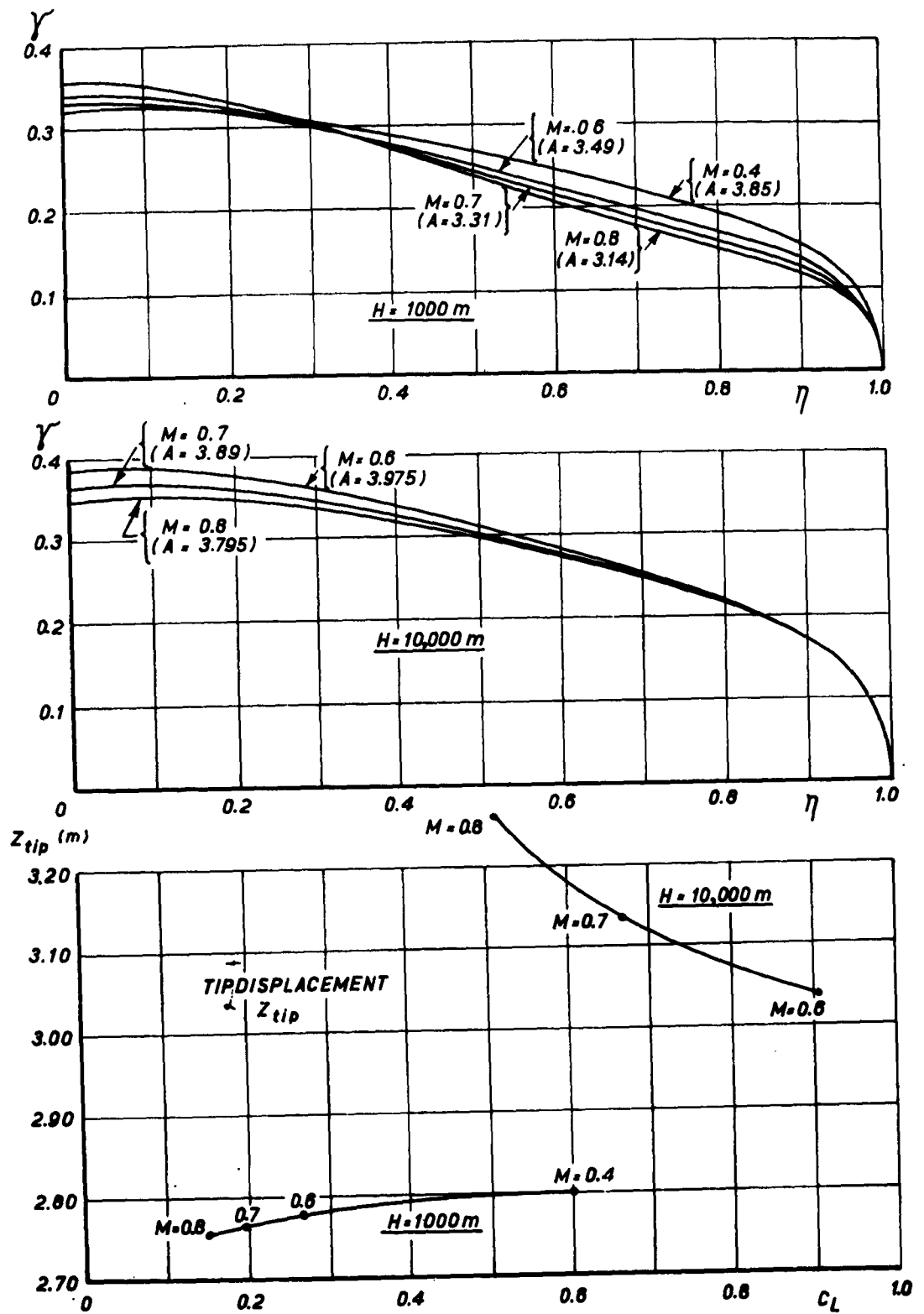


Fig. 11 Vertical displacement of wing tip with corresponding distributions of circulation

ADDENDUM

AGARD SPECIALISTS' MEETING

on

STABILITY AND CONTROL

Complete List of Papers Presented

Following is a list of the titles and authors of the 41 papers presented at the Stability and Control Meeting held in Brussels in April, 1960, together with the AGARD Report number covering the publication of each paper.

INTRODUCTORY PAPERS

- The Aeroplane Designer's Approach to Stability and Control*, by  
G.H.Lee (United Kingdom) .. .. . Report 334
- The Missile Designer's Approach to Stability and Control Problems*, by  
M.W.Hunter and J.W.Hindes (United States) .. .. . Report 335

DESIGN REQUIREMENTS

- Flying Qualities Requirements for United States Navy and Air Force Aircraft*, by W.Koven and R.Wasicko (United States) .. .. . Report 336
- Design Aims for Stability and Control of Piloted Aircraft*, by  
H.J.Allwright (United Kingdom) .. .. . Report 337
- Design Criteria for Missiles*, by L.G.Evans (United Kingdom) .. .. . Report 338

AERODYNAMIC DERIVATIVES

- State of the Art of Estimation of Derivatives*, by H.H.B.M.Thomas  
(United Kingdom) .. .. . Report 339
- The Estimation of Oscillatory Wing and Control Derivatives*, by  
W.E.A.Acum and H.C.Garner (United Kingdom) .. .. . Report 340
- Current Progress in the Estimation of Stability Derivatives*, by  
L.V.Malthan and D.E.Hoak (United States) .. .. . Report 341
- Calculation of Non-Linear Aerodynamic Stability Derivatives of  
Aeroplanes*, by K.Gersten (Germany) .. .. . Report 342

|   |            |
|---|------------|
| <i>Estimation of Rotary Stability Derivatives at Subsonic and Transonic Speeds</i> , by M.Tobak and H.C.Lessing (United States) .. .. .                               | Report 343 |
| <i>Calcul par Analogie Rhéoelectrique des Dérivées Aérodynamiques d'une Aile d'Envergure Finie</i> , by M.Enselme and M.O.Aguesse (France) ..                         | Report 344 |
| <i>A Method of Accurately Measuring Dynamic Stability Derivatives in Transonic and Supersonic Wind Tunnels</i> , by H.G.Wiley and A.L.Braslow (United States) .. .. . | Report 345 |
| <i>Mesure des Dérivées Aérodynamiques en Soufflerie et en Vol</i> , by M.Scherer and P.Mathe (France) .. .. .   | Report 346 |
| <i>Static and Dynamic Stability of Blunt Bodies</i> , by H.C.DuBose (United States) .. .. .   | Report 347 |

#### AEROELASTIC EFFECTS

|   |            |
|---|------------|
| <i>Effects of Aeroelasticity on the Stability and Control Characteristics of Airplanes</i> , by H.L.Runyan, K.G.Pratt and F.V.Bennett (United States) | Report 348 |
| <i>The Influence of Structural Elasticity on the Stability of Airplanes and Multistage Missiles</i> , by L.T.Prince (United States) .. ..             | Report 349 |
| <i>Discussion de deux Méthodes d'Etude d'un Mouvement d'un Missile Flexible</i> , by M.Bismut and C.Beatrice (France) .. .. .                         | Report 350 |
| <i>The Influence of Aeroelasticity on the Longitudinal Stability of a Swept-Wing Subsonic Transport</i> , by C.M.Kalkman (Netherlands) .. ..          | Report 351 |
| <i>Some Static Aeroelastic Considerations of Slender Aircraft</i> , by G.J.Hancock (United Kingdom) .. .. .   | Report 352 |

#### COUPLING PHENOMENA

|   |            |
|---|------------|
| <i>Pitch-Yaw-Roll Coupling</i> , by L.L.Cronvich and B.E.Amsler (United States)   | Report 353 |
| <i>Application du Calculateur Analogique à l'Etude du Couplage des Mouvements Longitudinaux et Transversaux d'un Avion</i> , by P.C.Haus (Belgium) .. .. .                        | Report 354 |
| <i>Influence of Deflection of the Control Surfaces on the Free-Flight Behaviour of an Aeroplane: A Contribution to Non-Linear Stability Theory</i> , by X.Hafer (Germany) .. .. . | Report 355 |

#### STABILITY AND CONTROL AT HIGH LIFT

|   |            |
|---|------------|
| <i>Low-Speed Stalling Characteristics</i> , by J.C.Wimpeny (United Kingdom) | Report 356 |
|---|------------|

|  |            |
|--|------------|
| <i>Some Low-Speed Problems of High-Speed Aircraft</i> , by A.Spence and D.Lean (United Kingdom) .. .. .                                | Report 357 |
| <i>Factors Limiting the Landing Approach Speed of an Airplane from the Viewpoint of a Pilot</i> , by R.C.Innis (United States) .. .. . | Report 358 |
| <i>Post-Stall Gyration and Their Study on a Digital Computer</i> , by S.H.Scher (United States) .. .. .                                | Report 359 |

**THE APPLICATION OF SERVO-MECHANISMS**

|   |            |
|---|------------|
| <i>The Place of Servo-Mechanisms in the Design of Aircraft with Good Flight Characteristics</i> , by K.H.Doetsch (United Kingdom) .. .. . | Report 360 |
| <i>Effects of Servo-Mechanism Characteristics on Aircraft Stability and Control</i> , by F.A.Gaynor (United States) .. .. .               | Report 361 |
| <i>Les Commandes de Vol Considérées comme Formant un Système Asservi</i> , by J.Grémont (France) .. .. .                                  | Report 362 |
| <i>Determination of Suitable Aircraft Response as Produced by Automatic Control Mechanisms</i> , by E.Mewes (Germany) .. .. .             | Report 363 |
| <i>An Approach to the Control of Statically Unstable Manned Flight Vehicles</i> , by M.Dublin (United States) .. .. .                     | Report 364 |

**THE USE OF SIMULATORS**

|   |            |
|---|------------|
| <i>The Use of Piloted Flight Simulators in General Research</i> , by G.A.Rathert, Jr., B.Y.Creer and M.Sadoff (United States) .. .. . | Report 365 |
| <i>Simulation in Modern Aero-Space Vehicle Design</i> , by C.B.Westbrook (United States) .. .. .                                      | Report 366 |
| <i>Mathematical Models for Missiles</i> , by W.S.Brown and D.I.Paddison (United Kingdom) .. .. .                                      | Report 367 |
| <i>In-Flight Simulation - Theory and Application</i> , by E.A.Kidd, G.Bull and R.P.Harper, Jr. (United States) .. .. .                | Report 368 |

**DEVELOPMENT TECHNIQUES**

|   |            |
|---|------------|
| <i>Application of Analytical Techniques to Flight Evaluations in Critical Control Areas</i> , by J.Weil (United States) .. .. .                 | Report 369 |
| <i>Investigation on the Improvement of Longitudinal Stability of a Jet Aircraft by the Use of a Pitch-Damper</i> , by R.Mautino (Italy) .. .. . | Report 370 |

*Méthodes Utilisées pour la Mise au Point de l'Avion Bréguet 940 à Ailes Soufflées*, by G. de Richemont (France) .. .. . **Report 371**

**TURBULENCE AND RANDOM DISTURBANCES**

*Theory of the Flight of Airplanes in Isotropic Turbulence; Review and Extension*, by B.Etkin (Canada) .. .. . **Report 372**

*The Possible Effects of Atmospheric Turbulence on the Design of Aircraft Control Systems*, by J.K.Zbrozek (United Kingdom) .. .. . **Report 373**

*L'Optimisation Statistique du Guidage par Alignement d'un Engin Autopropulsé en Présence de Bruit*, by P.LeFèvre (France) .. .. . **Report 374**

## DISTRIBUTION

Copies of AGARD publications may be obtained in the various countries at the addresses given below.

On peut se procurer des exemplaires des publications de l'AGARD aux adresses suivantes.

|                         |   |
|-------------------------|---|
| BELGIUM<br>BELGIQUE     | Centre National d'Etudes et de Recherches<br>Aéronautiques<br>11, rue d'Egmont, Bruxelles   |
| CANADA                  | Director of Scientific Information Service<br>Defense Research Board<br>Department of National Defense<br>'A' Building, Ottawa, Ontario       |
| DENMARK<br>DANEMARK     | Military Research Board<br>Defense Staff<br>Kastellet, Copenhagen Ø   |
| FRANCE                  | O.N.E.R.A. (Direction)<br>25, Avenue de la Division Leclerc<br>Châtillon-sous-Bagneux (Seine)   |
| GERMANY<br>ALLEMAGNE    | Wissenschaftliche Gesellschaft für Luftfahrt<br>Zentralstelle der Luftfahrtokumentation<br>München 64, Flughafen<br>Attn: Dr. H.J. Rautenberg |
| GREECE<br>GRECE         | Greek National Defense General Staff<br>B. MEO<br>Athens  |
| ICELAND<br>ISLANDE      | Director of Aviation<br>c/o Flugrad<br>Reykjavik  |
| ITALY<br>ITALIE         | Centro Consultivo Studi e Ricerche<br>Ministero Difesa-Aeronautica<br>Via dei Pontefici 3<br>Roma   |
| LUXEMBURG<br>LUXEMBOURG | Obtainable through Belgium  |
| NETHERLANDS<br>PAYS BAS | Netherlands Delegation to AGARD<br>Michiel de Ruyterweg 10<br>Delft   |

|                               |  |
|-------------------------------|--|
| NORWAY<br>NORVEGE             | Mr. O. Blichner<br>Norwegian Defence Research Establishment<br>Kjeller per Lilleström  |
| PORTUGAL                      | Col. J.A. de Almeida Viana<br>(Delegado Nacional do 'AGARD')<br>Direcção do Serviço de Material da F.A.<br>Rua da Escola Politecnica, 42<br>Lisboa |
| TURKEY<br>TURQUIE             | Ministry of National Defence<br>Ankara<br>Attn. AGARD National Delegate  |
| UNITED KINGDOM<br>ROYAUME UNI | Ministry of Aviation<br>T.I.L., Room 009A<br>First Avenue House<br>High Holborn<br>London W.C.1  |
| UNITED STATES<br>ETATS UNIS   | National Aeronautics and Space Administration<br>(NASA)<br>1520 H Street, N.W.<br>Washington 25, D.C.  |



*Prepared by Technical Editing and Reproduction Ltd  
95 Great Portland St. London, W.1.*

AGL (1) 6-63-1M-00003

|  |  |  |  |
|--|--|--|--|
| <p>AGARD Report 351<br/> North Atlantic Treaty Organization, Advisory Group<br/> for Aeronautical Research and Development<br/> <b>THE INFLUENCE OF AEROELASTICITY ON THE LONGITUDINAL<br/> STABILITY OF A SWEPT WING SUBSONIC TRANSPORT<br/> AIRCRAFT</b><br/> C. M. Kalkman<br/> 1961<br/> 36 pages incl. 7 refs., 11 figs; plus bibliography<br/> of papers presented at the Stability and Control<br/> Meeting</p> <p>A simplified numerical treatment of the influence<br/> of the aeroelastic deformations on the longitudinal<br/> stability and control characteristics of an air-<br/> craft with a swept-back wing of large aspect ratio</p> <p>P. T. O.</p> | <p>533.6.013.42<br/> 533.6.013.412<br/> 3c2c1a1<br/> 3c6b2</p> | <p>AGARD Report 351<br/> North Atlantic Treaty Organization, Advisory Group<br/> for Aeronautical Research and Development<br/> <b>THE INFLUENCE OF AEROELASTICITY ON THE LONGITUDINAL<br/> STABILITY OF A SWEPT WING SUBSONIC TRANSPORT<br/> AIRCRAFT</b><br/> C. M. Kalkman<br/> 1961<br/> 36 pages incl. 7 refs., 11 figs; plus bibliography<br/> of papers presented at the Stability and Control<br/> Meeting</p> <p>A simplified numerical treatment of the influence<br/> of the aeroelastic deformations on the longitudinal<br/> stability and control characteristics of an air-<br/> craft with a swept-back wing of large aspect ratio</p> <p>P. T. O.</p> | <p>533.6.013.42<br/> 533.6.013.412<br/> 3c2c1a1<br/> 3c6b2</p> |
| <p>AGARD Report 351<br/> North Atlantic Treaty Organization, Advisory Group<br/> for Aeronautical Research and Development<br/> <b>THE INFLUENCE OF AEROELASTICITY ON THE LONGITUDINAL<br/> STABILITY OF A SWEPT WING SUBSONIC TRANSPORT<br/> AIRCRAFT</b><br/> C. M. Kalkman<br/> 1961<br/> 36 pages incl. 7 refs., 11 figs; plus bibliography<br/> of papers presented at the Stability and Control<br/> Meeting</p> <p>A simplified numerical treatment of the influence<br/> of the aeroelastic deformations on the longitudinal<br/> stability and control characteristics of an air-<br/> craft with a swept-back wing of large aspect ratio</p> <p>P. T. O.</p> | <p>533.6.013.42<br/> 533.6.013.412<br/> 3c2c1a1<br/> 3c6b2</p> | <p>AGARD Report 351<br/> North Atlantic Treaty Organization, Advisory Group<br/> for Aeronautical Research and Development<br/> <b>THE INFLUENCE OF AEROELASTICITY ON THE LONGITUDINAL<br/> STABILITY OF A SWEPT WING SUBSONIC TRANSPORT<br/> AIRCRAFT</b><br/> C. M. Kalkman<br/> 1961<br/> 36 pages incl. 7 refs., 11 figs; plus bibliography<br/> of papers presented at the Stability and Control<br/> Meeting</p> <p>A simplified numerical treatment of the influence<br/> of the aeroelastic deformations on the longitudinal<br/> stability and control characteristics of an air-<br/> craft with a swept-back wing of large aspect ratio</p> <p>P. T. O.</p> | <p>533.6.013.42<br/> 533.6.013.412<br/> 3c2c1a1<br/> 3c6b2</p> |

is carried out for the sub-critical speed range. Only the deformation of the wing and the bending of the fuselage have been taken into consideration. As a result of the study it was found that the stability and control of the aircraft are only slightly affected by the aeroelastic deformation.

This Report is one in the Series 334-374, inclusive, presenting papers, with discussions, given at the AGARD Specialists' Meeting on 'Stability and Control', Training Center for Experimental Aerodynamics, Rhode-Saint-Genèse, Belgium, 10-14 April 1961, sponsored jointly by the AGARD Fluid Dynamics and Flight Mechanics Panels

is carried out for the sub-critical speed range. Only the deformation of the wing and the bending of the fuselage have been taken into consideration. As a result of the study it was found that the stability and control of the aircraft are only slightly affected by the aeroelastic deformation.

This Report is one in the Series 334-374, inclusive, presenting papers, with discussions, given at the AGARD Specialists' Meeting on 'Stability and Control', Training Center for Experimental Aerodynamics, Rhode-Saint-Genèse, Belgium, 10-14 April 1961, sponsored jointly by the AGARD Fluid Dynamics and Flight Mechanics Panels

is carried out for the sub-critical speed range. Only the deformation of the wing and the bending of the fuselage have been taken into consideration. As a result of the study it was found that the stability and control of the aircraft are only slightly affected by the aeroelastic deformation.

This Report is one in the Series 334-374, inclusive, presenting papers, with discussions, given at the AGARD Specialists' Meeting on 'Stability and Control', Training Center for Experimental Aerodynamics, Rhode-Saint-Genèse, Belgium, 10-14 April 1961, sponsored jointly by the AGARD Fluid Dynamics and Flight Mechanics Panels

is carried out for the sub-critical speed range. Only the deformation of the wing and the bending of the fuselage have been taken into consideration. As a result of the study it was found that the stability and control of the aircraft are only slightly affected by the aeroelastic deformation.

This Report is one in the Series 334-374, inclusive, presenting papers, with discussions, given at the AGARD Specialists' Meeting on 'Stability and Control', Training Center for Experimental Aerodynamics, Rhode-Saint-Genèse, Belgium, 10-14 April 1961, sponsored jointly by the AGARD Fluid Dynamics and Flight Mechanics Panels